Earth-Science Reviews 234 (2022) 104216

Contents lists available at ScienceDirect

Earth-Science Reviews

journal homepage: www.elsevier.com/locate/earscirev

Aerosol-cloud interactions over the Tibetan Plateau: An overview

Yuzhi Liu [a], Jianping Huang [a,b,*], Tianhe Wang [a], Jiming Li [a], Hongru Yan [a], Yongli He [a]

[a] Key Laboratory for Semi-Arid Climate Change of the Ministry of Education, College of Atmospheric Sciences, Lanzhou University, Lanzhou 730000, China

[b] Land–atmosphere Interaction and its Climatic Effects Group, State Key Laboratory of Tibetan Plateau Earth System, Resources and Environment (TPESRE), Institute of Tibetan Plateau Research, CAS, Beijing 100101, China

ARTICLE INFO

Keywords:
Tibetan Plateau
Aerosol
Cloud
Precipitation
Interaction

ABSTRACT

This paper reviews progress in the study of aerosol-cloud interactions over the Tibetan Plateau (TP) in the past decade. Clarifying the aerosol-cloud-precipitation interactions over the TP is an important issue for both local and downstream precipitation forecasts. By exerting a "dynamic pump" effect due to the elevated heat source in summer, the TP acts as a "transfer station" for aerosols and water vapor, possessing abundant water vapor and enough cloud condensation nuclei (CCN) and ice nuclei (IN) in cloud physical processes. We found that mixtures of aerosols and clouds are frequently observed over the margin areas of the TP, especially the mixture between aerosols and ice clouds. The convective clouds over the TP could be affected by the Taklimakan dusts lifted from the north slope of the TP, inducing higher and more invigorated convective clouds locally. Furthermore, the dust-polluted convective clouds can continuously move eastward and merge with the convective cloud clusters along their motion paths, inducing more intensive rainfall over the downstream regions of the TP. Finally, challenges to further understanding aerosol-cloud interactions over the TP in the future are discussed.

1. Introduction

The Tibetan Plateau (TP), which is also called the "Asian water tower", supplies freshwater for 40% of the world's population (Immerzeel et al., 2010) due to its expansive water storage, such as glaciers, lakes, and rivers. During the last three decades, the TP has been experiencing accelerated warming compared to the global mean (Duan and Xiao, 2015; Wang et al., 2008; Yao et al., 2012), making the TP at risk of directly melting snow and glaciers. For the Asian water tower, rainfall is the unique supply process maintaining the hydrological balance. Generally, the evolution of precipitation takes on a variety of forms and involves numerous physical processes; these processes are dependent upon the characteristics of the aerosol loading in addition to the vertical motion of air within clouds, the liquid-water production of clouds, the turbulence structure, and the time scales of clouds (Twomey et al., 1984; Cotton and Yuter, 2009). Therefore, cloud- and precipitation-related studies are important for understanding the changes in and mechanisms of the Asian water tower, concerning the survival of billions of people in the world.

Moreover, it has long been known that the TP is the "Roof of the World" with an average elevation of 4000 m above sea level (ASL) and an area of approximately 2.5×10^6 km^2. Generally, large-scale mountain ranges have been assigned crucial roles in shaping the regional and even global climate by mechanical and thermal dynamical effects (Molnar

Abbreviations: AA, Anthropogenic aerosol; ACI, Aerosol-Cloud Interaction; AOD, Aerosol Optical Depth; ATAL, Asian Tropopause Aerosol Layer; ATM, Atmosphere; BC, Black Carbon; CALIPSO, Cloud-Aerosol Lidar and Infrared Pathfinder Satellite Observations; CCN, Cloud Condensation Nuclei; CERES, Clouds and the Earth's Radiant Energy System; CESM, Community Earth System Model; CMIP5, Coupled Model Intercomparison Project Phase 5; CRF, Cloud Radiative Forcing; ET, EvapoTranspiration; EOS, Earth Observation Satellite; ERBE, Earth Radiation Budget Experiment; *EASM*, *East Asian Summer Monsoon*; GD, Gurbantunggut Desert; GITD, Great Indian Thar Desert; GTDL, Global Tropopause Dust Layer; IC, Indo-China; ICDR, Ice Cloud Droplet Radius; IN, Ice Nuclei; IPCC, Intergovernmental Panel on Climate Change; ISCCP, International Satellite Cloud Climatology Project; IRF, Indirect Radiative Forcing; IWC, Ice Water Content; IWP, Ice Water Path; MISR, Multi-angle Imaging SpectroRadiometer; MODIS, Moderate-resolution Imaging Spectroradiometer; NICAM, Nonhydrostatic Icosahedral Atmospheric Model; SPRINTARS, Spectral Radiation-Transport Model for Aerosol Species; SASM, *South Asian Summer Monsoon*; SAT, Surface Air Temperature; SFC, Surface; SWJ, Subtropical Westerly Jet; TCW, Total Column Water Vapor; TD, Taklimakan Desert; TOA, Top of the Atmosphere; TP, Tibetan Plateau; TRMM, Tropical Rainfall Measuring Mission; UTLS, Upper Troposphere and Lower Stratosphere; WRF-Chem, Weather Research and Forecasting coupled with chemistry.

* Corresponding author at: Key Laboratory for Semi-Arid Climate Change of the Ministry of Education, College of Atmospheric Sciences, Lanzhou University, Lanzhou 730000, China.

E-mail address: hjp@lzu.edu.cn (J. Huang).

https://doi.org/10.1016/j.earscirev.2022.104216
Received 5 August 2022; Received in revised form 4 October 2022; Accepted 8 October 2022
Available online 14 October 2022

et al., 2010; Wu et al., 2012; Wu et al., 2015; Boos and Kuang, 2010). Due to the elevated land surface and thus enhanced sensible heating, the TP acts as a raised heat source in spring and summer (Yanai et al., 1992; Wu and Zhang, 1998; Wu et al., 2007). Such a thermal structure facilitates the virtual functionality of the TP serving as an "air pump", attracting warm and moist air from low-latitude oceans (Wu et al., 2012). Consequently, an isolated region of humidity has formed in the atmosphere over the TP (Xu et al., 2008), playing an important and special role in the global energy-water cycle.

The abundant water vapor that benefits from the TP "heat-driving air pump" provides one of the necessary conditions to form clouds. Fundamentally, clouds over the TP are strongly influenced by the special thermodynamic features in summer owing to the large scale of the plateau and its extreme topography (Luo and Yanai, 1984; Xu et al., 2013). Clouds have profound effects on both weather and climate by adjusting the radiation budget of the atmosphere and affecting the water cycle via precipitation (Liou, 1986; Rossow and Schiffer, 1999). Moreover, many studies have reported that the easterly outflow of water vapor and clouds away from the TP can contribute significantly to precipitation over downstream regions (Wan et al., 2017). Thus, studies on the TP could provide potential clues for promoting the predictability of downstream weather and climate.

The TP is at the juncture of several important natural and anthropogenic aerosol sources and is surrounded by the Earth's highest mountains, including the Himalayas and the Pamir and Kunlun ranges, with the Taklimakan Desert (TD) to the north, the Gobi Desert to the northeast and the Great Indian Desert (GITD) to the southwest. With the increasing frequency of dust storms nearby (Thulasiraman et al., 2002; Uno et al., 2001), the TP faces new threats due to the influence of aerosols. Aerosols can scatter and absorb a fraction of the incoming solar radiation to influence the temperature and atmospheric stability (Jacobson, 2002). In addition, aerosols also serve as cloud condensation nuclei (CCN) or ice nuclei (IN), modifying cloud properties and precipitation (Twomey, 1977; Penner et al., 2001; Rosenfeld et al., 2014). However, the impacts of aerosols on cloud properties constitute one of the largest uncertainties in climate predictions (Boucher et al., 2013), and the knowledge of aerosol impacts over the TP is much poorer.

Our research on the aerosol-cloud interactions (ACI) and related issues has significantly advanced in recent years, leading to a better understanding of how aerosols and clouds can contribute to TP climatic changes and how aerosols interact with clouds to further influence local and downstream rainfall. This paper summarizes a brief overview of aerosol-cloud topics based mainly on recent studies by research groups. We will review the progresses in optical and radiative properties of aerosols over the TP in Section 2, the properties of clouds and their impacts on climate over the TP in Section 3, the ACI over the TP and its impact on local and downstream precipitation in Section 4. The summary and outlook on the aerosol-cloud over the TP are presented in Section 5. Finally, an abbreviation list is given in Section 6.

2. Aerosol properties and radiative effect over the TP

Aerosols are small particles suspended in the atmosphere (Ramanathan et al., 2001;), comprising a mixture of mainly sulfate, soil dust, carbonaceous material, and sea salt. Aerosols can affect the Earth's climate system by altering the radiative properties of the atmosphere directly through scattering and absorbing solar radiation (Charlson et al., 1992; Miller and Tegen, 1998) and can also affect cloud properties (Ackerman et al., 2000; Huang et al., 2006a; Huang et al., 2006b; Huang et al., 2010; Twomey, 1974; Twomey et al., 1984) to indirectly influence the radiation budget. Many studies were carried out on the optical and radiative properties in the region to the northeast of TP (e.g., Wang et al., 2010; Bi et al., 2011; Che et al., 2019a), in the region to the northwest of TP (e.g., Liu et al., 2011; Wang et al., 2021b; Yang et al., 2021), and in the region to the south of TP (e.g., Mehta et al., 2021), providing some evidences for aerosol source and transportation over the TP.

2.1. Distribution properties over the TP

Due to the immense topography of the TP, averaging >4000 m in elevation, few ground-based measurements, including cascade impactor aerosol sampling (e.g., Zhang et al., 2001) and polycarbonate filter sampling (e.g., Cong et al., 2007), have been performed. Since the 1980s, taking advantage of satellites, an increasing amount of aerosol information has been collected to compensate for the scarcity of ground-based measurements on the TP (e.g., Xu et al., 2015). In 2006, the Cloud-Aerosol Lidar and Infrared Pathfinder Satellite Observations (CALIPSO) satellite was launched into orbit around Earth as part of the "A-Train", a constellation of Earth-observing satellites, providing valuable information about the altitudes of aerosol layers in the atmosphere. Additionally, based on reliable observational data as a verification of the simulation ability of models, numerical models have also been shown to provide some high-spatial-temporal resolution transportation information.

On the whole, the atmosphere over the TP is minimally disturbed by anthropogenic activities due to the sparse population and limited industries. For example, it was reported that a very low annual aerosol optical depth (AOD) was measured on the central TP (Cong et al., 2009). However, the TP is located close to South and East Asia, where the largest sources of dust and carbonaceous aerosols in the world are distributed. Therefore, widespread air pollution can enter the interior TP through atmospheric circulation (Xia et al., 2008; Cong et al., 2013).

Regarding long-term dust events and loading over the TP, most studies have been based on ice records (e.g., Kang et al., 2000; Wang et al., 2006). Meanwhile, Chinese meteorological station observations on the TP have provided information on dust events, including dust storms, blowing dust and floating dust records, with daily resolution over the long term (Kang et al., 2016). CALIPSO reveals that dust storms occur more frequently than were previously found from Tibetan surface observations because few surface sites were available over remote northwestern Tibet due to the high elevation and harsh climate. Tibetan dust layers appear most frequently approximately 4–7 km above mean sea level (Huang et al., 2007), and some layers are lofted to altitudes of 10 km and higher (Liu et al., 2008). Recently, it has continually been reported that dust is the most prominent aerosol type on the TP through sampling (Duo et al., 2015) and Multi-angle Imaging Spectroradiometer (MISR) and CALIPSO satellite observations (Xu et al., 2015; Jia et al., 2015; Liu et al., 2015).

In addition, anthropogenic aerosols (AAs), including carbonaceous aerosols and sulfate, have also been found over the TP (Liu et al., 2015; Zhang et al., 2015; Zhao et al., 2017; Zhang et al., 2021). Especially over the eastern slope of the TP, the AOD is extremely large and can be even larger than that in some important industrialized regions and deserts; the main aerosol component over the eastern slope of the TP is sulfate, followed by carbonaceous aerosols (Jia et al., 2019). Employing 10-year (2007–2016) space-based active and passive measurements, Wang et al. (2020) found that the TP has been regularly exposed to polluted air masses with significant amounts of absorbing aerosols (Fig. 1).

2.2. Source and transport of TP aerosols

Geographically, the TP is bounded by Asian drylands to the west and north and the Indian subcontinent to the south. The TP is located at the junction of natural aerosol sources, including the TD, Gobi Desert and GITD, and anthropogenic pollution sources. Based on a statistical analysis performed for the period from 2007 to 2014, Jia et al. (2015) concluded that Tibetan dusts are mainly sourced from the TD and partially from the Gurbantunggut Desert (GD) and the GITD (Fig. 2). It was found that, for the Northeast Region (area A as shown Fig. 2), TD is the main dust source, accountsing for 65% of the detected dust events. The GD and Kumtag deserts both account for 32% of the dust events over

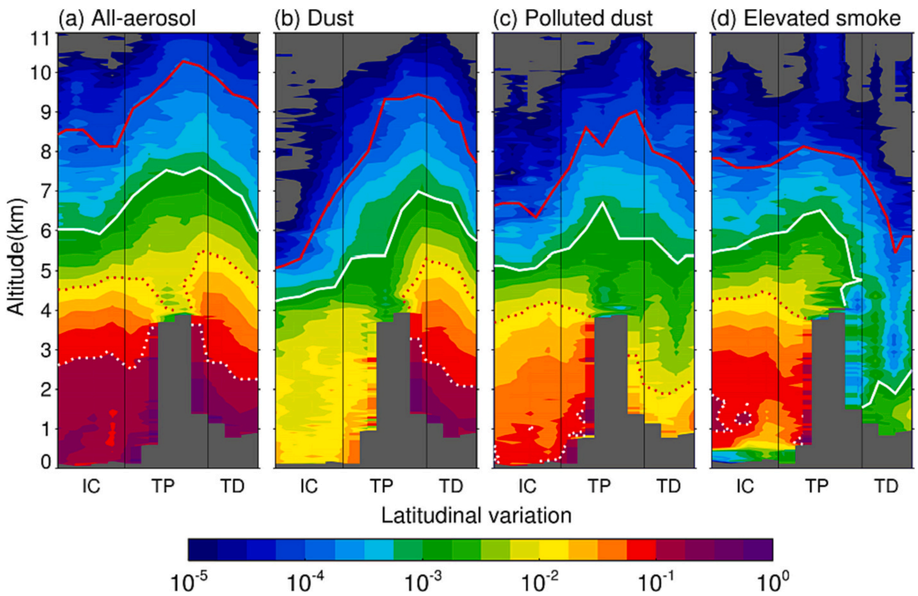

Fig. 1. Latitudinal variations in the decadal mean aerosol extinction coefficients (km^{-1}) for (a) all-aerosol, (b) dust, (c) polluted dust, and (d) elevated smoke over the Indo-China (IC) (19–27°N), TP (27–37°N), and TD (37–43°N) subregions (from Wang et al., 2020). The red solid lines, white solid lines, red dotted lines, and white dotted lines denote the heights with aerosol extinction of 0.0001, 0.001, 0.01, and 0.1 km^{-1}, respectively. (For interpretation of the references to colour in this figure legend, the reader is referred to the web version of this article.)

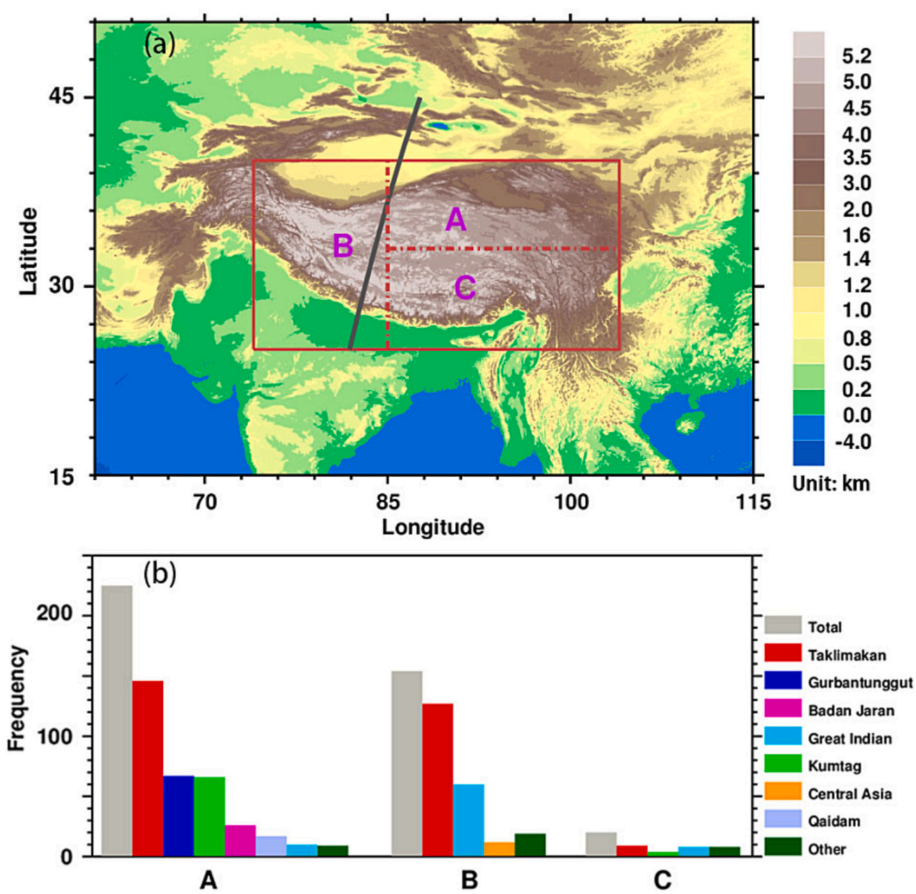

Fig. 2. (a) Topographical distribution over the TP. The TP is divided into three parts (separated by the crimson dotted lines): the Northeast Region (area **A**: 33–40°N, 85–105°E), Western Region (area **B**: 25–40°N, 70–85°E) and Southeast Region (area **C**: 25–40°N; 70–85°E). The thick dark gray line indicates the orbit path of CALIPSO over the TP on 15 June 2009. **(b)** Frequencies (number of occurrences) of dust events occurring in summertime over the three regions of the TP from 2007 to 2014. The gray bars present the total frequencies of dust occurrences, and the colorized bars present the frequencies of sources corresponding to the detected dust events (Reproduced from Jia et al., 2015).

the area A, and the Badain Jaran and Qaidam deserts both account for approximately 3% of the events. For the Western Region (area B in Fig. 2), the neighboring TD and GITD account for 84% and 40% of the detected dust events, respectively. Because there may be two or more sources for a certain dust event, the sum of the percentages for a region is not equal to 100%. Besides, the dust aerosols during events seldomly occurring over the Southeast Region (area C in Fig. 2) originate from the neighboring TD and GITD.

Many studies have explored both the zonal (e.g., Lau and Kim, 2010; Liu et al., 2015; Chen et al., 2017b) and meridional (e.g., Xu et al., 2020; Hu et al., 2020) transports of aerosols over the TP. Past studies found that during spring and summer, there exists a dust belt with a high AOD extending eastward from the TD to the Loess Plateau along the Hexi Corridor and southward to the TP (Ge et al., 2014). It was reported that the changes in regional aerosol optical depth may greatly contributed by the meteorological factors (Che et al., 2019b) as well as large-scale circulation system. Yumimoto et al. (2009) indicated that the strong northeasterly surface winds associated with low pressures invading the TD through the eastern corridor can form strong upslope winds along the high, steep mountainsides of the TP and blow large amounts of dust into the air. In summer, the meridional transport of TD dusts to the TP is favored by the thermal effect of the TP and the weakening of East Asian westerly winds. A TD dust flux arrived at the TP with a value of 6.6 Gg/day in the study event but decayed quickly during southward migration over the TP due to dry deposition (Chen et al., 2013). Jia et al. (2015) revealed that when a cold advection or front developed by strong cold advection passes, dust particles are emitted into the atmosphere from the TD and GD and then transported to the northern slope of the TP with northeasterly winds induced by the Altai and Tian Shan mountains. Combining the Spectral Radiation-Transport Model for Aerosol Species (SPRINTARS) coupled with a nonhydrostatic regional model, Liu et al. (2015) further provided evidence of the Tibetan dust distribution and transport features. Moreover, a regional model study with a tracer-tagging technique also confirmed the transport of dust from surrounding sources (Hu et al., 2020). Additionally, it was also reported that the increased atmospheric dust over the TP is caused by two aspects: (1) higher dust emissions over the Middle East and (2) enhanced mid-latitude zonal winds that help transport more dust in the middle troposphere from central Asia to Northwest China (Feng et al., 2020).

In addition, much of the TP dust mobilized from the GITD is associated with passing low-pressure system activity and is generally polluted by AAs (Jia et al., 2015). Based on a typical dust event analysis, the entire Indian-Gangetic Plain, southern India, the Bay of Bengal, and even the TP can be influenced by dust events (Wang et al., 2021b). One studied dust storm was caused jointly by an upper-level jet stream, an upper trough and the subtropical high. A typical south-north secondary circulation adjacent to its exit zone, mainly triggered by the upper-level jet stream, promoted much stronger and higher vertical uplift of the dust aerosols over the Thar Desert. Consequently, those uplifted dust particles were easily transported to the TP across the majestic Himalayas by the southerly airflows in front of the low-pressure trough over Afghanistan and the southern branch trough over Bengal Bay (Fig. 3).

Additionally, the massive topography of the TP plays an important role in dust transportation via topographic effects. According to CALIPSO observations, an "airborne dust corridor", extending from west to east, shows seasonality largely modulated by the TP through its dynamical and thermal forcing effects on atmospheric flows (Liu et al., 2008). Through Tibetan topography experiments performed using the Weather Research and Forecasting coupled with chemistry (WRF-Chem) model, Tan et al. (2021) revealed that the existence of Tibetan topography can change the near-surface wind speeds by adjusting the atmospheric circulations, in turn changing the dust emission location in the TD and strengthening dust emissions in the GITD and Gobi Desert.

Moreover, when a dust event occurs, we found that the AAs entrained into the southwesterly current via the Indian summer monsoon are transported from India to the southern slope of the TP (Ji et al., 2015). Simultaneously, abundant AAs are also transported from eastern China to the east of the TP by easterly winds (Liu et al., 2015). Concerning AAs transport over the TP, many potential mechanisms have been proposed. Yuan et al. (2020) reported that the weakness of westerly wind over the northern TP, acceleration of westerly wind over the southern TP, and the eastward shift of the East Asia major trough are responsible for the high BC concentrations measured over the east slope of the TP. At the global scale, it was considered that the winter loss of Arctic sea ice over the subpolar North Atlantic could boost aerosol transport toward the TP in April, when aerosol loading is at its climatological maximum preceding the onset of the Indian summer monsoon (Li et al., 2020). Of course, similar to dust transportation over the TP, AAs transport is also significantly affected by the TP topography.

Furthermore, the TP acts as a "transfer station", vertically redistributing the accumulated dust aerosols. In recent years, in situ measurements have successively revealed some robust evidences of aerosols extending above the tropopause (Tobo et al., 2007; Yu et al., 2017; Zhang et al., 2020). Moreover, it has been reported that mineral dust is the dominant aerosol by mass in the Asian Tropopause Aerosol Layer (ATAL), showing large interannual variabilities but no long-term trend due to its natural variability (Bossolasco et al., 2021; Yuan et al., 2019). Some studies have also provided evidence of dust aerosol transport through the TP to the upper troposphere and lower stratosphere (UTLS) (Xu et al., 2018). Regarding the mechanism by which vertical pollutants are transported to the stratosphere, Lau and Kim (2010) proposed that monsoon circulation can provide an effective pathway by which pollution from Asia, India, and Indonesia can enter the global stratosphere. In addition, Pan et al. (2016) showed that the intraseasonal east–west oscillation of the anticyclone may play an essential role in transporting convectively pumped boundary layer pollutants in the UTLS.

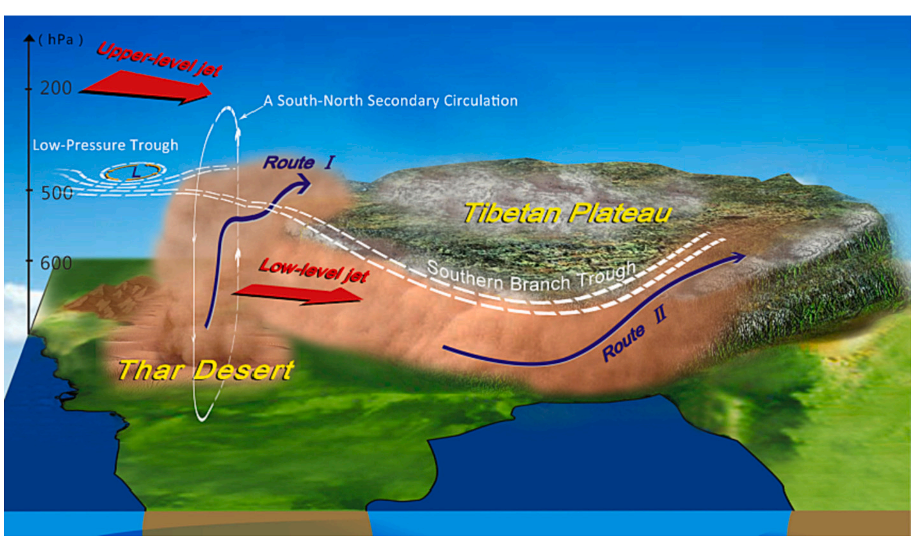

Fig. 3. A schematic diagram of the transport mechanism of dust aerosols over South Asia to the TP. The red arrows represent the upper-level jet stream at 200 hPa and the low-level jet stream at 600 hPa. The white directional circle indicates the vertical secondary circulation triggered by the upper-level jet stream. The white dashed lines symbolize the atmospheric flow fields at the 500-hPa level. The blue arrows represent the two transport routes to the TP (complied from Wang et al., 2021b).

Quantitatively, a three-dimensional aerosol transport-radiation model combined with a global model proved that the TP is an important transport pathway of the global tropopause dust layer (Zhu et al., 2021). It was reported that large amounts of dust at relatively low layers can be transported to the southwestern slope of the TP, where the updrafts are the strongest, causing the southwestern slope of the TP to become the strongest transport pathway. The northern slope of the TP also accumulates dust aerosols, but this transport pathway is weak due to the relatively weak local updrafts (Fig. 4). In addition, deep convection can also inject dust aerosols into the stratosphere. It has also been proven that enhanced transport to the ATAL resulting from overshot deep convection can be observed over preferred pathways in the Himalayan-Gangetic Plain and the Sichuan Basin (Yuan et al., 2019). Additionally, it has been considered that the aerosol abundances in the upper troposphere and lower stratosphere are associated with the Asian summer monsoon (Lau et al., 2018; Ma et al., 2019; Niu et al., 2019; Bian et al., 2020).

Additionally, past work has revealed that in the UTLS, carbonaceous aerosols, including black carbon (BC) and organic carbon (OC), and sulfate aerosols were also found in addition to dust aerosols (Fadnavis et al., 2013; Lau et al., 2018). Bossolasco et al. (2021) quantified that the aerosols other than dust in the ATAL are composed of approximately 40% sulfate, 30% secondary and 15% primary organic aerosols, 14% ammonium aerosols and <3% BC. Furthermore, Yu et al. (2016) pointed out that the organic material in the lowermost stratosphere contributes 30–40% of the nonvolcanic stratospheric AOD. Aircraft in situ measurements suggested that the carbonaceous and sulfate aerosols at relatively low ATAL altitudes are largely supplied by deep convection over the Indian subcontinent through the transport of pollution into the UTLS (Vernier et al., 2015).

2.3. Radiative effect of aerosols over the TP

Generally, the radiative effects of aerosols over the TP include two aspects. Some studies have focused on the first, direct effects, which are induced by suspended aerosols absorbing and scattering the solar radiation and thermal radiation emitted by the Earth-atmosphere system (e.g., Jia et al., 2018; Fadnavis et al., 2017). In addition, some studies have focused on the effects of aerosols on snow or glaciers and have concluded that absorbing aerosols, such as dust and BC deposited on glaciers and snow, can reduce the surface albedo, thus accelerating glacier and snow melt (Qin et al., 2000; Xu et al., 2007; Qian et al., 2011; Li et al., 2017). In the following text, we will emphatically discuss the radiative effects of aerosols suspended in the atmosphere.

It has been pointed out that dust aerosols transported from nearby deserts in northern India can heat the air over the southern slope of the TP, leading to an advanced onset and intensification of the Indian summer monsoon (Lau and Kim, 2006). Coupled with BC, dust-induced atmospheric heating can lead to 6%–10% snowpack cover reductions over the western TP and Himalayan regions (Lau and Kim, 2010). Therefore, the direct effects of aerosols on the radiation balance and temperature over the TP are nonnegligible in TP climate research.

It has been estimated that over the TP, the direct radiative forcing induced by dust aerosols was -1.28 Wm^{-2} (cooling) at the top of the atmosphere (TOA), 0.41 Wm^{-2} (warming) in the atmosphere, and -1.68 Wm^{-2} (cooling) at the surface during the 2010–2015 period (Hu et al., 2020). Moreover, some studies have provided some estimates of the direct radiative effect of TP dust aerosols through case studies. Chen et al. (2013) estimated that the event-averaged net radiative forcings of TD dust over the TP are 3.97 Wm^{-2}, 1.61 Wm^{-2}, and 5.58 Wm^{-2} at the TOA, in the atmosphere, and at the surface, respectively. By recalculating the aerosol extinction coefficient derived from the CALIPSO observations over the TP, Jia et al. (2018) estimated the instantaneous radiative forcing by dust aerosols over the TP. Overall, dust aerosols significantly affect the radiative energy budget and thermodynamic structure of the air over the TP, mainly by altering the shortwave radiation budget. The instantaneous heating rate can be as high as 5.5 K/day depending on the density of the dust layers (Fig. 5).

Simultaneously, carbonaceous aerosols can alter the aerosol radiation balance by -4.74 ± 1.42 Wm^{-2}, $+0.37 \pm 0.26$ Wm^{-2} and $+5.11 \pm 0.83$ Wm^{-2} at the surface, at the TOA and in the atmosphere, respectively, over the TP and Indo-Gangetic Plain region (15–35°N, 80–110°E) (Fadnavis et al., 2017). Based on the intraseasonal dry–wet phase transition over the southeastern TP, Yang et al. (2018) found that an

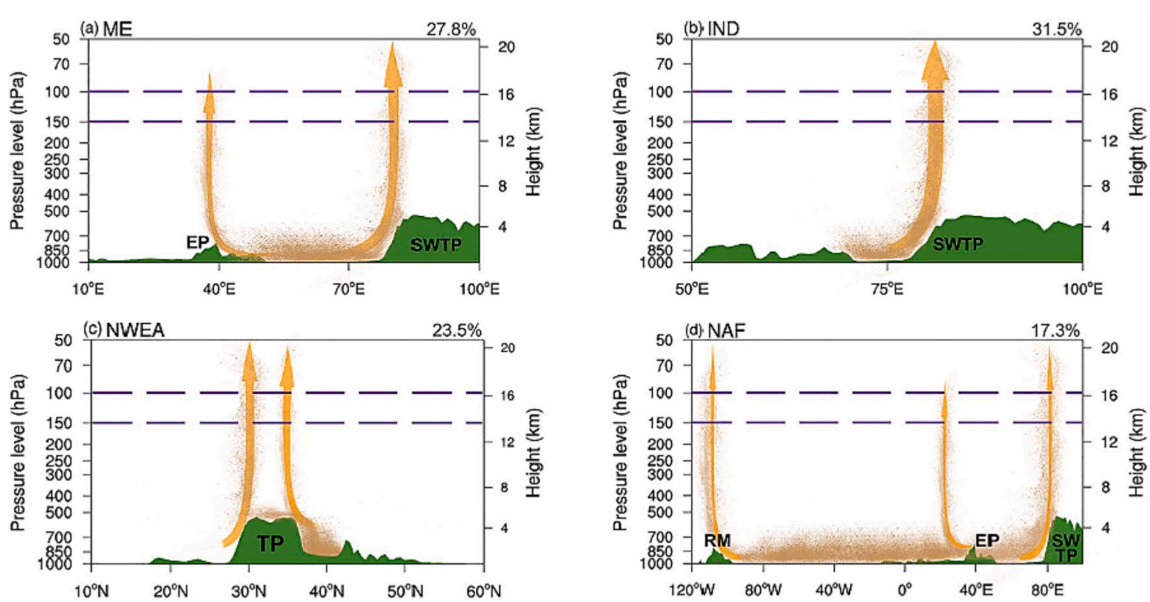

Fig. 4. Schematic illustration of the transport of dust to the global tropopause dust layer (GTDL). Transport of dust originating from (a) the Middle East (ME), (b) the Indian Peninsula (IND), (c) northwestern East Asia (NWEA), and (d) North Africa (NAF) to the GTDL (complied from Zhu et al., 2021). The yellow arrows represent the transport pathways, and the numbers in the upper left corners represent the contributions of the dust sources to the GTDL at 100 hPa. EP represents the Ethiopian Plateau, SWTP represents the southwestern slope of the TP and RM represents the Rocky Mountains. The green shading indicates the topographic elevation. The purple lines denote the 100 and 150 hPa layers. (For interpretation of the references to colour in this figure legend, the reader is referred to the web version of this article.)

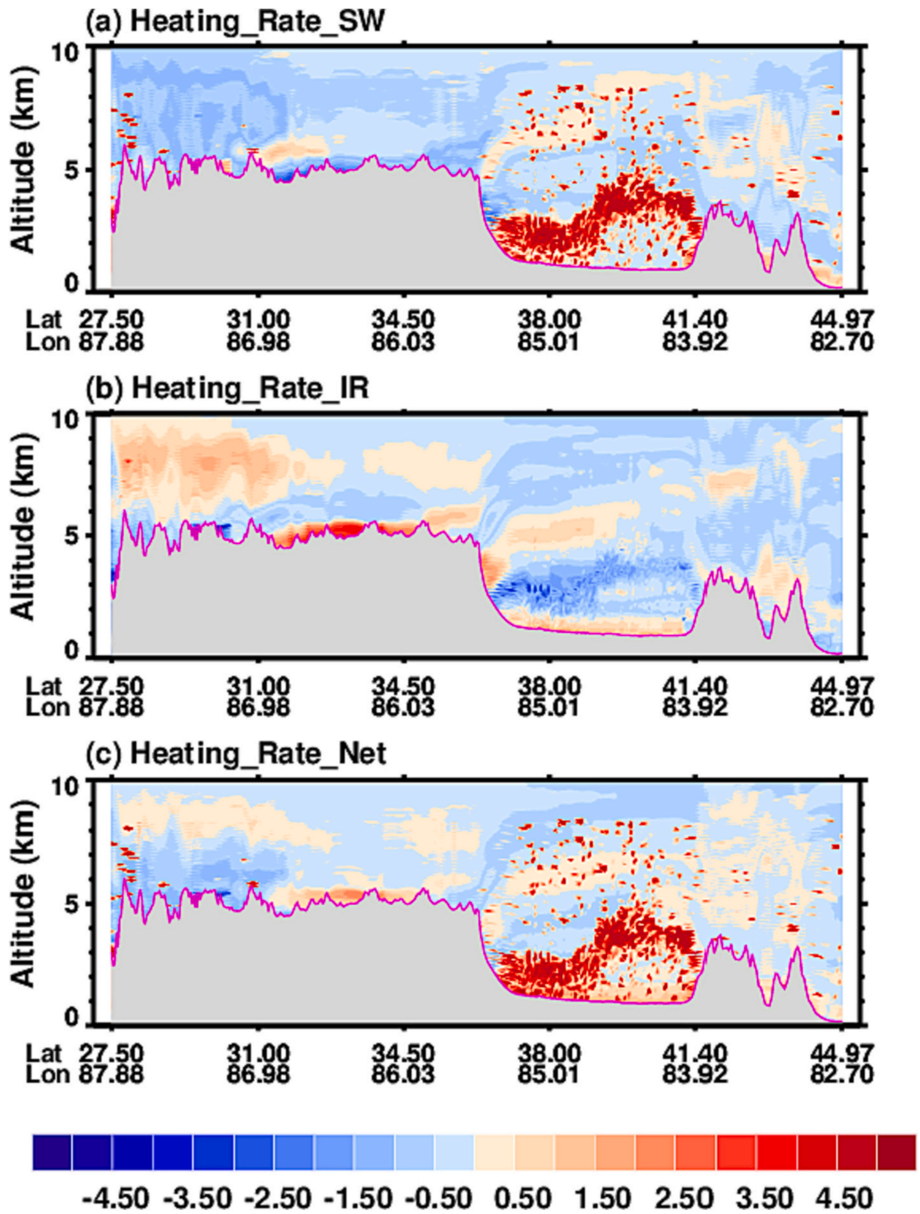

Fig. 5. Altitude-orbit cross-sections of (a) shortwave, (b) infrared and (c) net heating rates (units: K/day) due to the presence of aerosols along the CALIPSO orbit path over the TP on 07 August 2008 (from Jia et al., 2018). The unit is K/day. The light gray section indicates the topography. The pink curve denotes the surface. (For interpretation of the references to colour in this figure legend, the reader is referred to the web version of this article.)

increase in the observed local BC concentration of >50% led to approximately 4 Wm^{-2} of atmospheric radiative warming and approximately 2 Wm^{-2} of surface radiative cooling. In addition, the radiative effect of carbonaceous aerosols in the monsoon season is different from that in the nonmonsoon season. In the nonmonsoon season, carbonaceous aerosols can increase surface air temperatures by 0.1–0.5 °C over the TP but decrease temperatures in South Asia during the monsoon season (Ji et al., 2015). Jiang et al. (2017) presented that the TP warming-induced increase in BC induces an intensification of the East Asian winter monsoon northern mode, under which conditions the BC is mostly transported from northern South Asia by wintertime westerlies and southwesterlies.

Additionally, the aerosols transported to the UTLS could also exert some impacts on the Earth-atmosphere system radiation budget and temperature. It has been reported that near-global satellite aerosol data imply negative radiative forcing due to stratospheric aerosol changes over this period of approximately −0.1 Wm^{-2}, reducing the recent global warming that would otherwise have occurred (Solomon et al., 2011). Vernier et al. (2015) reported that the Asian tropopause aerosol layer exerted a short-term regional forcing at the top of the atmosphere of −0.1 Wm^{-2} during the 2006–2013 period. A small amount of BC in the stratosphere could significantly increase the radiative forcing, but observations are presently lacking to support this (Boucher et al., 2013). Through model simulations, Yu et al. (2016) estimated an aerosol radiative forcing of −0.072 Wm^{-2} in the stratosphere since 1850; this value is approximately 21% of the aerosol direct radiative forcing of the full depth of the atmosphere estimated by the Intergovernmental Panel on Climate Change (IPCC) (Boucher et al., 2013). The authors found a higher contribution of stratospheric aerosols to radiative forcing (21%) than to AOD change (12%) since 1850. However, it was shown that near-surface BC causes surface warming, whereas near-tropopause BC and BC in the stratosphere cause surface cooling (Ban-Weiss et al., 2012; Samset and Myhre, 2015; Mills et al., 2014).

3. Cloud properties over the TP

Before the "satellite meteorology" era of the 1980s, knowledge of clouds over the TP was very limited and was largely based on measurements from a very limited number of surface meteorological stations (e.g., Uyeda et al., 2001; Ueno et al., 2001; Xu et al., 2002; Li et al., 2008; Zhou et al., 2009; He et al., 2013; Liu et al., 2015; Chang et al., 2019; Zhou et al., 2021). With the satellite-launch process after the 1980s, cloud data measured by multiple satellites have been accumulated for many years over the TP (e.g., Li et al., 2006; Naud and Chen, 2010; Luo et al., 2011; Rüthrich et al., 2013). Based on satellite images, it was revealed that there exists some relationship between cloud activity and topography over the TP and surrounding areas (Ueno, 1998; Yasunori and Fujio, 2002). Complex factors including topography discrepancy could induce smaller range in the variation of cloud thickness and cloud top height corresponding to different precipitation intensity (Yan et al., 2016), relatively weak deep convective systems with convective intensity and small size but frequent occurrence (Qie et al., 2014), and different precipitation characteristics (e.g., Hu et al., 2010; Cai et al., 2021) over the TP than its neighboring region. On the whole with the increased number of obtained observations, the features of TP clouds have been gradually revealed.

3.1. Water vapor supply for cloud formation

According to previous studies, four primary atmospheric circulation systems regulate moisture transport to the TP, including the Indian monsoon system, the midlatitude westerlies, the East Asian monsoon system and the local moisture recycling termed the "Tibetan Plateau monsoon" (Duan et al., 2011; Xu et al., 2008; Yao et al., 2012; Ma et al., 2018). Overall, the supply of moisture to TP precipitation is modulated by the above circulation systems. Statistically, within the main region contributing 90% of the moisture-causing precipitation in the TP, the moisture supplied from the lands and oceans at proportions above 69% and 21%, respectively (Zhang et al., 2017). It has been reported that the TP continuously attracts the upwards movement of warm and moist air from low-latitude oceans (Wu et al., 2012); the moisture from the Indian Ocean and the Bay of Bengal dominates the summer precipitation in the southeastern TP (Feng and Zhou, 2012, Zhang et al., 2021). Consequently, a large amount of moisture can climb over the TP and supply abundant water vapor for cloud and precipitation formation.

In recent decades, with the extreme sensitivity of the TP climate to global warming (Duan and Wu, 2006, Duan et al., 2018; Ma et al., 2017), the water vapor transport process over the TP has correspondingly changed. By using the European Centre for Medium-Range Weather Forecasts interim reanalysis data collected during the 1979–2014 period, Zhou et al. (2019) found that the water vapor over the TP in summer experienced an interdecadal variation around the middle of the 1990s with a drier phase during the 1979–1994 period and a subsequent wetter phase. Based on an investigation of the long-term changes in atmospheric water vapor balance across the TP from 1979 to 2018, Yan et al. (2020) found that the water vapor convergence close to Yarlung Zangbo Grand Canyon exhibited a sharp decrease. Simultaneously, the Brahmaputra Basin, inner TP, and southern Qilian Mountain have exhibited significant wetting tendencies (Fig. 6). In addition, from the moisture balance perspective, it was further proven that moisture convergence tended to increase over the western TP but decrease over the eastern TP from 1979 to 2019 (He et al., 2021). Consequently, changes in the water vapor budget over the TP are closely related to cloud formation and precipitation and thus influence the water storage of the "Asian water tower".

Generally, the regional feature of water vapor balance across the TP is a result of complex factors, including atmospheric heat sources (Yang et al., 2014; Duan et al., 2018), wind stilling (Ma et al., 2017), and atmospheric circulation from high-latitude regions (Zhou et al., 2019; Xu and Gao, 2019). He et al. (2021) proposed a mechanism to explain the coupling effect between the internal and external water cycles over the TP (Fig. 7). The authors considered that an increase in the atmospheric heating source over the western TP could shift the transport of moisture from east to west at the southern boundary of the TP. This increasing moisture convergence could enhance precipitation, and the enhanced latent heating in the mid-atmosphere could further induce moisture convergence, forming a positive feedback effect.

Apart from the above factors, it has been reported that atmospheric particles could also influence water vapor transport to the TP through radiative effects. It has been suggested that the radiative effect of BC can

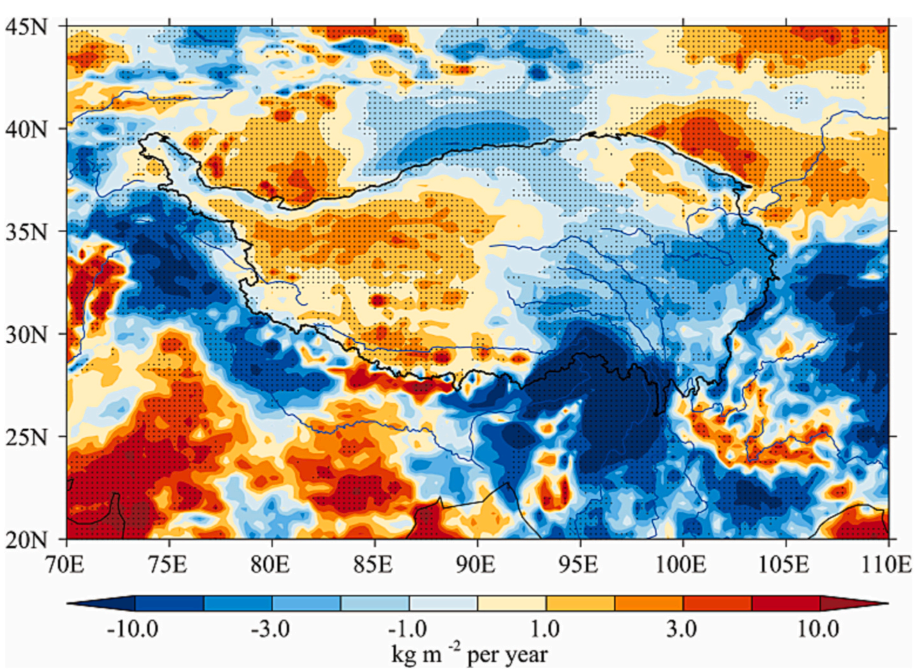

Fig. 6. Horizontal distribution of the long-term (1979–2018) trend in the vertical integrated divergence of annual water vapor fluxes (unit: kg m^{-2} $year^{-1}$) over the TP (reproduced from Yan et al., 2020).

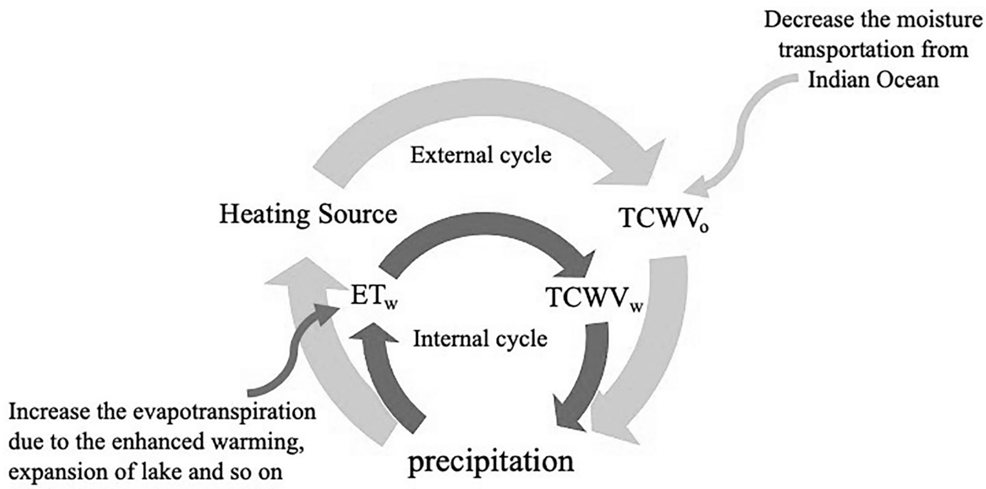

Fig. 7. Schematic illustration of the coupling effect between the internal and external water cycles over the TP (from He et al., 2021). ET denotes evapotranspiration, and TCWV indicates total column water vapor. Subscripts *w* and *o* represent the water vapor that evaporates within the region and outside the region, respectively.

induce an updraft motion with a warm anticyclone circulation in the upper atmosphere over the TP in late spring or early summer (Lau and Kim, 2006, 2010). Based on the simulation for the summer from 2001 to 2005 by the Community Earth System Model (CESM), Luo et al. (2020) pointed out that BC can induce a pronounced warming effect over the TP and consequently intensify the East Asian summer monsoon (EASM). However, significant cooling effects in northern India, Pakistan, Afghanistan and Iran are induced due to BC and its related feedbacks, thus significantly reducing the meridional land–sea thermal contrast and finally weakening the South Asian summer monsoon (SASM). Consequently, the water vapor transport to the south border is decreased due to the addition of BC. Overall, by affecting atmospheric circulation, BC can induce an increase in the amount of water vapor imported from the west and east borders of the TP and an increase in the amount of water vapor outflowing away from the north border of the TP (Fig. 8).

3.2. Cloud properties and changes

The preliminary radar observations obtained in the second Tibetan Plateau Experiment of atmospheric science (TIPEX-II) at Naqu station over the TP showed that convective clouds were mostly column cells and that "popcorn-like" convective clouds were frequently detected (Xu et al., 2002). Moreover, Doppler radar observations obtained at Naqu station revealed that summertime clouds exhibited obvious diurnal variation associated with strong solar radiation heating over the TP (Uyeda et al., 2001; Liu et al., 2002; Zhou et al., 2009; Liu et al., 2015). Aircraft measurements conducted around the Naqu station over the TP demonstrated that the summertime clouds over the TP were primarily characterized as mixed-phase cumulus clouds induced by strong solar radiation heating (Chang et al., 2019). Overall, from ground-based observations, previous studies have shown that the TP is an active region of summer convective systems (Li et al., 2008). Convective activities over the TP often rapidly intensify after noon and reach their maxima in early evening (Fujinami and Yasunari, 2001). Daytime precipitation is often related to scattered, small-scale convective monomers, while nighttime precipitation is associated with large-scale stratiform clouds in the Naqu basin of the TP (Ueno et al., 2001). Additionally, associated with convective clouds, ice clouds were also simultaneously observed by Lidar at the Naqu station (He et al., 2013). On the TP, cloud property measurements have also been reported at other stations, for example, Motuo National Climate Observatory (Zhou et al., 2021) and Lhasa (Tobo et al., 2007), and at some sites in the vicinity of the TP (Ge et al., 2017, 2018, 2019).

In addition to ground-based measurements, satellite observations are an efficient way of obtaining cloud properties over the TP. Many comparisons or assessments of the TP cloud properties observed by multiple satellites (Li et al., 2006; Naud and Chen, 2010; Luo et al., 2011; Rüthrich et al., 2013) have been performed. Furthermore, comparisons between the satellite observations and reanalysis data, including assimilated observations (including ground-based and satellite

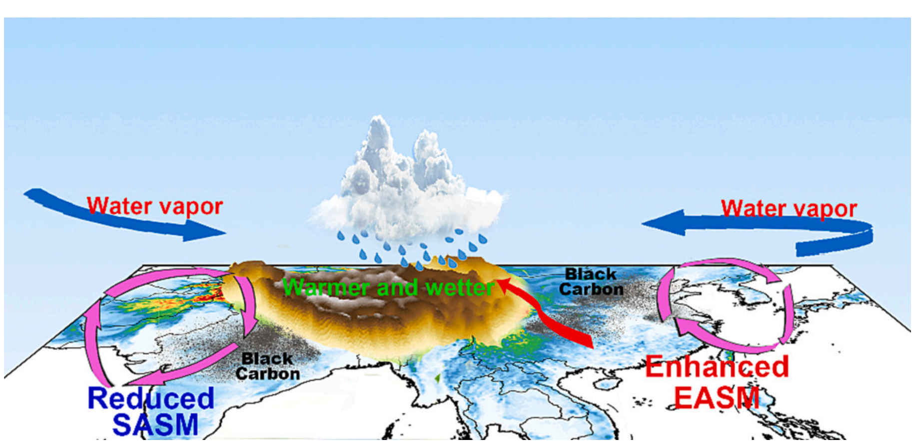

Fig. 8. Mechanism by which BC affects water vapor transport over the TP (from Luo et al., 2020). EASM and SASM indicate the East Asian summer monsoon and South Asian summer monsoon, respectively.

measurements) and model simulations, have been demonstrated (You et al., 2014; Lei et al., 2020). Satellite observations from the Earth Radiation Budget Experiment (ERBE) showed that on the eastern flank of the TP, the annual mean cloud optical depth exhibits a maximum in the global tropics and extratropics (between 60°S and 60°N) (Yu et al., 2004). In accordance with the detection of ice clouds by ground-based measurements (He et al., 2013), the Earth Observation Satellite (EOS) (Li et al., 2005), combination of CloudSat and CALIPSO satellite data (Luo et al., 2011; Li and Zhang, 2016), and Tropical Rainfall Measuring Mission (TRMM) satellites have also frequently detected cirrus clouds composed of ice crystals and partially associated with deep convective clouds (Qie et al., 2014; Fu et al., 2006). Additionally, multi-satellite observations also detected a strong diurnal cycle over the TP (Fujinami and Yasunari, 2001; Yasunori and Fujio, 2002; Shang et al., 2018), which is consistent with ground-based measurements (Uyeda et al., 2001; Liu et al., 2002; Zhou et al., 2009) and numerical model simulations (Sato et al., 2008). Combining four-year (2007–2010) cloud phase products from CloudSat and CALIPSO, Wang et al., 2021a further provided some evidence for using ground-based measurements (Chang et al., 2019) to determine that ice clouds frequently occur during the cold season (CS), while the mixed-phase cloud fraction is more frequent during the warm season (WS). Moreover, similar conclusions based on Moderate-resolution Imaging Spectroradiometer (MODIS) data have been obtained (Gao et al., 2003; Chen and Liu, 2005). Consistently, Liu et al. (2019a) pointed out that compared to water clouds, ice clouds were observed more frequently from 2000 to 2016; this was proven by cloud-resolving models (Sato et al., 2007; Chen et al., 2017a). Based on Clouds and Earth's Radiant Energy System (CERES) satellite observations, ice clouds have been reported to be mainly distributed over the TP margin area during both daytime and nighttime. The occurrence frequency of ice clouds, which is defined as the number of ice-cloudy sky divided by the total sample number in each grid, is higher during the daytime than during the nighttime over the marginal areas of the TP (Fig. 9).

In recent years, with enhanced warming over the TP, it has been reported that cloud properties have changed. Based on 6-hourly weather observations collected at 71 stations across the central and eastern TP from 1961 to 2003, it has been reported that the low-level cloud amount exhibits a significant increasing trend during nighttime; on the other hand, both the total and low-level cloud amounts tend to decrease during daytime (Duan and Wu, 2006). These variations in cloud type may further affect surface warming on the TP. Furthermore, the cloud amounts observed at 75 stations on the TP were analyzed (Zhang et al., 2008), and the authors found that over the past decades, the total cloud amount has shown an obviously declining tendency. Using satellite observations from 2000 to 2015, Hua et al. (2018) found that the middle-level cloud fraction (middle cloud) decreased (−0.36%/year), while the high-level cloud fraction (high cloud) increased (+0.24%/year) over almost the entirety of the TP during the CS.

3.3. Radiative effects of clouds on the Tibetan climate

Clouds may influence the Earth's climate by modulating the radiation budget (Hartmann et al., 1992; Ramanathan et al., 2001). On the one hand, clouds can scatter solar radiation, much of which returns to space, resulting in "cloud albedo forcing" taken by itself and a resulting cooling effect on Earth. On the other hand, a cloud can absorb the longwave radiation emitted by the Earth-atmosphere system, resulting in the "cloud greenhouse effect" taken by itself and a resulting warming effect on Earth (Sohn et al., 2010; Zelinka et al., 2013). Consequently, the net effect of clouds depends on the competition result of cloud albedo forcing and the greenhouse effect. In general, low, thick water clouds exert net cooling on the Earth due to the predominance of cloud albedo forcing by reflecting much of the solar radiation, while high, thin cirrus clouds result in net warming of the Earth due to the cloud greenhouse forcing being greater than the albedo effect. Thus, different cloud properties induce different cloud effects (Slingo, 1989).

Generally, the effects of clouds on the radiation budget are quantified by cloud radiative forcing (CRF), which represents the difference between cloud-free radiative fluxes and the averages of all-sky observations (Coakley and Baldwin, 1984; Ramanathan et al., 1989). Overall, the CRF at the TOA is dominated by cooling effects over the TP, the distribution of which is mainly determined by the shortwave CRF (Su et al., 2000; Yan et al., 2016). Specifically, Wang et al., 2021a estimated the cloud radiative effects (CRE) of different phase clouds at the TOA, surface (SFC), and atmosphere over the TP (Fig. 10). They concluded

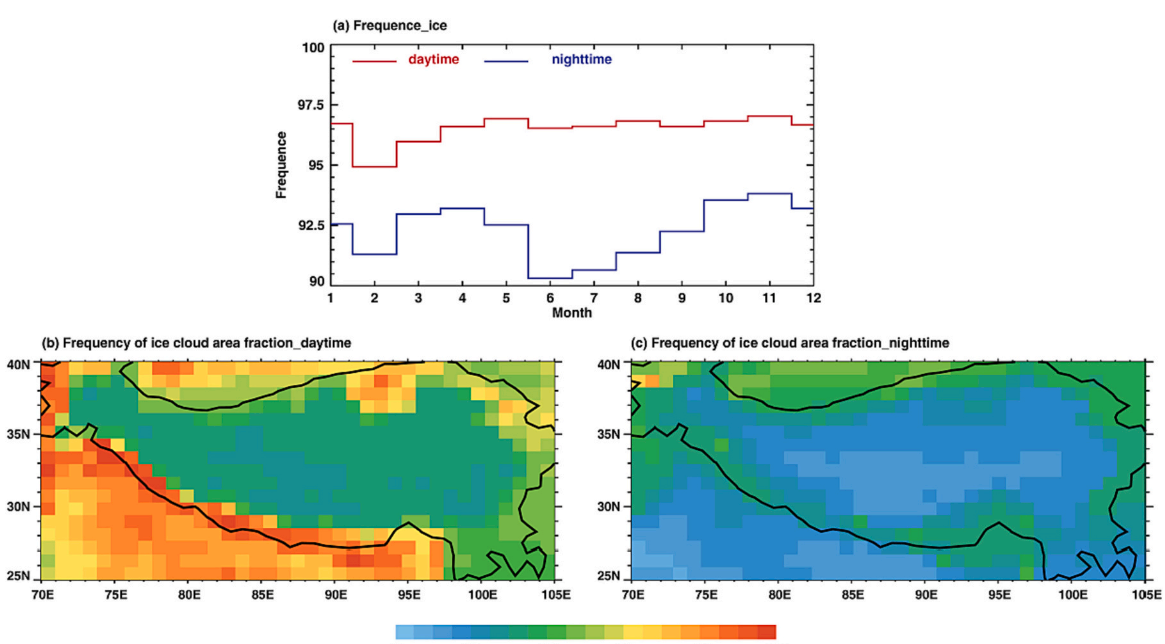

Fig. 9. (a) Monthly mean histogram of ice cloud area fractions (unit: %) during the 2000–2015 period. (b) Frequency (unit: %) of the annual ice cloud area fraction in daytime over the TP during the 2000–2015 period. Panel (c) is the same as (b) but for nighttime (from Liu et al., 2019a). The area enclosed by the black curve indicates the main body of the TP.

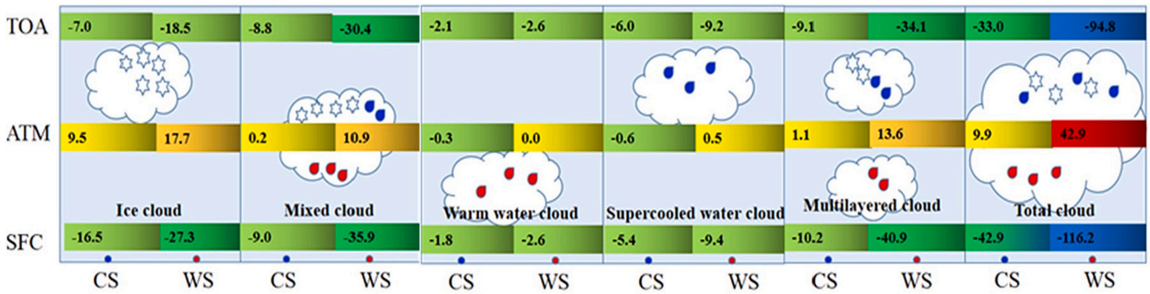

Fig. 10. Four-year (2007–2010) CRE (unit: Wm^{-2}) of ice clouds, mixed-phase clouds, supercooled water clouds, warm water clouds, multilayered clouds, and total clouds at the TOA, atmosphere (ATM), and surface (SFC) over the TP. The left-to-right values of each cube indicate the CRE of different cloud phases during the CS and WS. The small spheres of different colors above each line represent different seasons, with blue and red representing the CS and WS, respectively. The first four different cloud phases refer to cases of single-layer clouds (from Wang et al., 2021a). (For interpretation of the references to colour in this figure legend, the reader is referred to the web version of this article.)

that the clouds at both the TOA and SFC exhibited colling effects. The strongest cooling effect of the total clouds was found during the WS, with effects of approximately −116.2 Wm^{-2} and -94.8 Wm^{-2} at the SFC and TOA, respectively. Moreover, these findings indicate that the strong heating effect resulting from clouds in the atmosphere during the WS is mainly caused by ice and missed-phase and multilayered clouds, while liquid clouds contribute lesser effects.

It has been claimed that the radiative effect of clouds is more important than other factors over the TP (Sun, 1995). Duan and Wu (2006) reported that a significant increase in low-level cloud amounts across the central and eastern TP could enhance downward atmospheric radiation and weaken effective terrestrial radiation, leading to strong nocturnal surface warming from 1961 to 2003. On the other hand, both the total and low-level cloud amounts during the daytime have displayed decreasing trends, resulting in increased absorption of direct solar radiation at the surface and associated surface warming. Based on satellite and reanalysis datasets, Yang et al. (2012) pointed out that solar dimming over the TP region is mainly due to the increased water vapor amount and deepened cloud cover, which in turn are related to rapid warming and the increased convective available potential energy. By using CERES satellite observations and the Coupled Model Intercomparison Project Phase 5 (CMIP5) model simulations, Hua et al. (2018) found that, due to an increase in high-cloud amounts and a decrease in middle-cloud amounts over most parts of the TP, the decreased albedo effect of middle clouds and the increased longwave greenhouse effect of high clouds may have partially contributed to the sustained warming effect, especially during the CSs from 2000 to 2015. Moreover, these results indicate that the warming rate and cloud property changes are significantly amplified with elevation.

4. Aerosol-cloud interactions and their impacts on precipitation

Aerosols can affect the temperature and alter the atmospheric stability by scattering or absorbing a fraction of radiation (Jacobson, 2002; Wang et al., 2013), thus indirectly exerting an influence on cloud formation and properties. Moreover, aerosols serve as CCN or IN, thus modifying cloud optical properties and lifetimes. The impacts of aerosols on cloud properties have constituted one of the largest uncertainties in climate predictions (Forster et al., 2021). Moreover, the effect of aerosols on precipitation has been regarded as an important but poorly understood process (Levin and Cotton, 2007).

4.1. Features of aerosol-cloud interactions over the TP

Considering the high quality of data covering 2007–2010, Liu et al. (2019a) analyzed the frequency distribution of the aerosol and ice cloud mixture by using CALIPSO and CloudSat observations collected during the 2007–2010 period. The results indicate that the mixture frequency of aerosols and ice clouds is higher over the marginal areas of the TP than over the central TP (Fig. 11). Therefore, the possibility of aerosol-cloud interactions exists due to the presence of this mixture.

The association between aerosols and clouds over the TP has been evaluated in previous studies. Combining satellite data from CALIPSO and CloudSat, Pan et al. (2018) presented the impact of dust aerosols on the microphysical properties of cirrus clouds over the TP. The authors reported that due to the existence of dust aerosols, the ice water content (IWC), ice water path (IWP), ice distribution width, ice effective radius, and ice number concentration decreased by 17%, 18%, 4%, 19%, and 10%, respectively. Based on satellite observations and reanalysis datasets, it was found that with the AOD increasing to its peak, the ice particle size decreased to a minimum, and convective clouds developed to increased heights because of the prolonged cloud life (Liu et al., 2019b). In addition, the authors found that potential relationships may exist between the aerosol index (defined as the product of the AOD and Angström exponent) and ice cloud properties. When the aerosol index increased from 0.05 to 0.17, the daytime ice cloud droplet radius (ICDR) decreased from 32.1 to 27.9 μm, while the nocturnal ICDR remained almost constant (at approximately 25 μm); furthermore, the daytime IWP decreased slightly due to the saturation effect, while the nocturnal IWP increased significantly (Liu et al., 2019a).

Simultaneously, focusing on the relations between aerosols and clouds over the TP, numerical simulations have been performed with regional and global models. Based on a cloud-resolving model, Zhou et al. (2017) found that an increased aerosol concentration generally enhances the cloud core updraft and maximum updraft, thus intensifying convections in cumulus clouds over the TP and leading to increased precipitation with aerosol concentrations. Using the SPRINTARS model coupled with the Nonhydrostatic Icosahedral Atmospheric Model (NICAM), Liu et al. (2020) further provided numerical evidence for Taklimakan dusts affecting the convective cloud properties over the TP. Hua et al. (2020) compared and quantified the inconsistent aerosol indirect effects on the properties of water clouds and ice clouds by using CMIP5 model results over the TP. The effect of aerosols on the radiative forcing of ice clouds is more significant than that on the forcing of water clouds, for which the aerosol indirect effect is dominated by the effect on the shortwave radiative forcing of ice clouds. The CMIP5 simulation results suggest that the aerosol indirect effect on the total radiative forcing of water clouds over the TP is −0.34 (±0.03) Wm^{-2}, while that on the forcing of ice clouds is −0.73 (±0.03) Wm^{-2} (Fig. 12).

Additionally, Tobo et al. (2007) proposed the occurrence of selective ice nucleation involving a fraction of background aerosols (i.e., effective ice nuclei) using balloon-borne optical particle counters; this process is associated with dynamical and constituent fields in the upper troposphere over the TP. In addition, the aerosol type, a major contributor to ice-nucleating particles in mixed-phase clouds, differs among different temperatures; for example, biological particles are major contributors at

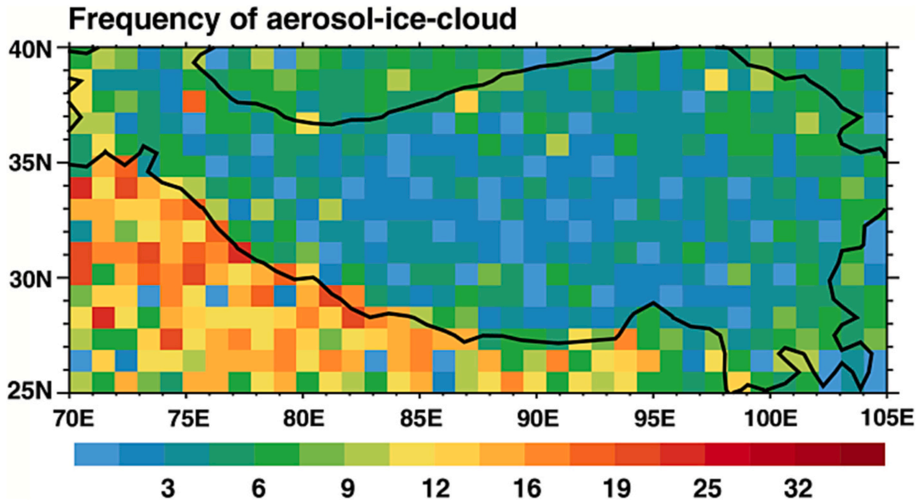

Fig. 11. Frequency (unit: %) distribution of the aerosol and ice cloud mixture obtained from CALIPSO and CloudSat observations obtained over the TP from 2007 to 2010 (reproduced from Liu et al., 2019a). The area enclosed by the black curve indicates the main body of the TP.

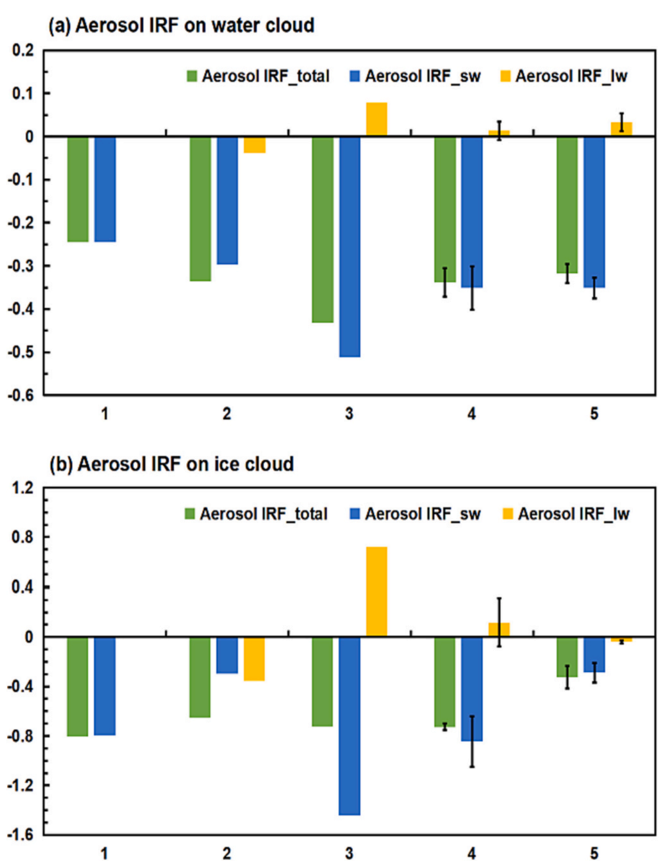

Fig. 12. Aerosol total indirect radiative forcing (IRF) (green bar), shortwave IRF (blue bar), and longwave IRF (yellow bar) on (a) water clouds and (b) ice clouds simulated by models (numbers 1, 2, and 3 correspond to the Hadley Centre Global Environment Model version 2 (HadGEM2-A), Model for Interdisciplinary Research on Climate version 5 (MIROC5), and Meteorological Research Institute-Coupled Global Climate Model version 3 (MRI-CGCM3), respectively; number 4 represents the multimodel ensemble mean) and calculated from MISR and CERES satellite data (number 5) (complied from Hua et al., 2020). Error bars represent the standard errors of the multimodel ensemble means. Subscripts *sw* and *lw* denote short wave and longwave, respectively. (For interpretation of the references to colour in this figure legend, the reader is referred to the web version of this article.)

temperatures above −20 °C over the TP (Chen et al., 2021). Therefore, considering the complex atmospheric composition over the TP, the uncertainties in aerosol-cloud interactions need to be considered.

4.2. Impact of aerosol-cloud interactions on precipitation on the TP and downstream

Previous studies have shown that cloud and precipitation processes are easily affected in relatively clean atmospheric environments (Garrett and Zhao, 2006; Zhao et al., 2020). Relatively, the aerosol loading over the TP is much lower than those over other regions, thus leading to the more sensitive response of precipitation to aerosol-cloud interactions.

Han et al. (2009) proposed that there were significant negative correlations between dust aerosols and precipitation in dust source regions during both the 1961–2000 and 1800–2000 periods. It was found that the role of precipitation in suppressing dust storms could be unimportant, while dust aerosols may play an important role in suppressing precipitation in the hinterland of the TP (Han et al., 2009). In addition, the relations between precipitation and carbonaceous aerosols were investigated. It has been hypothesized that the current warming may enhance the emissions of biogenic volatile organic compounds that can increase secondary organic aerosols, thus contributing to an increase in precipitation (Fang et al., 2015).

Zhou et al. (2017) found that the precipitation in cumulus clouds over the TP increases with aerosol concentrations, thus not only facilitating precipitation but also transporting more ice-phase hydrometeors into the upper troposphere and decreasing the precipitation efficiency. Considering the very clean atmosphere over the TP, elevated aerosol concentrations can remarkably enhance convections due to the specific underlying topography, and this process could influence the Asian summer monsoon. Moreover, previous studies have already revealed that absorbing aerosols over the TP have been proposed to directly affect monsoon rainfall through the elevated-heat-pump mechanism (Lau et al., 2008; Luo et al., 2020). Recently, the spatial correlation of the daily AOD with cloud properties and precipitation during both wet and dry monsoonal years indicated a positive association of relatively high aerosol concentrations with cloud vertical development and precipitation. The 0 °C isotherm was found to be higher by 136.82 ± 18.82 m (mean ± standard deviation) during polluted days than in relatively clean environments, and this may be crucial in affecting changes in the snow line and glacial melting, thus impacting the hydroclimate of the Himalayas (Adhikari and Mejia, 2021).

The aerosol-cloud interactions over the TP not only influence precipitation on the TP but also contribute to downstream precipitation

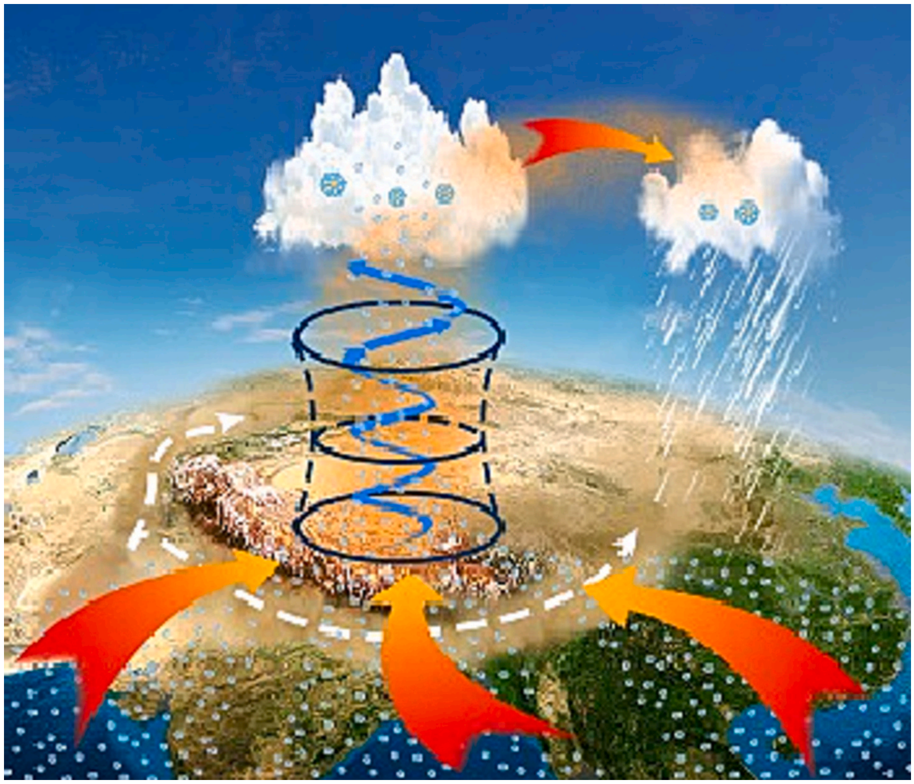

Fig. 13. Schematic of aerosol-cloud interactions and impacts on precipitation over the TP.

(Fig. 13). Based on the analysis and simulation of an aerosol-cloud interaction event over the TP (Liu et al., 2019b; Liu et al., 2020), we found that convective clouds polluted by Taklimakan dust over the northern slope of the TP continuously move eastward and merge with convective cloud clusters along the motion path, thus inducing significant precipitation over the downstream regions of the TP. In addition, Liu et al. (2020) proposed a dynamic northern drought mechanism attributable to the TP in summer. The meridional shift in the subtropical westerly jet (SWJ) is the determining factor of the northern summertime drought. When the SWJ shifts northward, the upper-level westerly wind is weakened; thus, the water vapor, clouds or dusty clouds over the TP are transported to the north less often, reducing precipitation and causing more frequent droughts. In contrast, when the SWJ shifts southward, the northern area of China experiences increased summertime precipitation.

5. Summary and outlook

In this paper, we reviewed the aerosol-cloud properties and interactions over the TP. In particular, our studies during the last decade have systematically emphasized the aerosol distribution features and transport mechanisms, cloud properties, aerosol-cloud interactions over the TP and their impacts on local and downstream precipitation. Some findings have been summarized as follows.

Dust is the dominant aerosol type over the TP and is mainly sourced from the Taklimakan Desert and partially from the GD and GITD. Serving as a "transfer station" of dust aerosols, the TP plays an important pathway by which dust is transported to the UTLS, thus contributing the dominant aerosol by mass in the ATAL. In addition, AAs, including carbonaceous and sulfate aerosols, have been observed in the atmosphere and snowpack. Dust and carbonaceous aerosols over the TP could exert a cooling effect at the surface but a warming effect in the atmosphere; this is closely related to the altitude of the aerosol layer. Acting as a large, elevated heat source in summertime due to its massive topography, the TP continuously attracts warm and moist air from surrounding oceans through the "dynamic pump" effect, supplying abundant water vapor for cloud formation. It has been reported that water vapor presented an increase over the western TP but a decrease over the eastern TP during the period from 1979 to 2019; over the same period, the water vapor close to Yarlung Zangbo Grand Canyon exhibited a sharp decrease. Ice clouds are frequently observed over the TP margin area, especially over the northern slope; this is consistent with the aerosol index distribution. Moreover, these findings indicate that the mixture frequency of aerosols and ice clouds is relatively high over the marginal areas of the TP. The aerosol effect on the radiative forcing of ice clouds is more significant than that on the forcing of water clouds, in which the aerosol indirect effect is dominated by the effect on the shortwave radiative forcing of ice clouds. Convective clouds, which are polluted by Taklimakan dusts over the north slope of the TP, continuously move eastward and merge with the convective cloud clusters along their motion paths, thus inducing significant precipitation over the downstream regions of the TP.

Despite great progress, many questions remain unresolved, and challenges remain in the following aspects. Observations are very important for the study of aerosol-cloud interactions; however, there is currently a lack of adequate data for accurately understanding the features of interactions between aerosols and clouds over the TP. Because of the complicated topography of the TP, the precision, content, and coverage of satellite datasets and in situ observations still cannot satisfy the requirements of current studies. Obvious errors also exist in data representing aerosol properties and aerosol-cloud mixtures, inducing immense uncertainties when calculating the radiative effects of aerosols and the impacts of aerosols on clouds. To fully understand the aerosol-cloud interactions over the TP, it is necessary to establish more aerosol and cloud observation stations over the TP, particularly for data-scarce regions in the northwestern TP and at high elevations. Regarding the impacts of aerosols on clouds determined from observational analyses, some impacts are partially contributed by other factors, such as meteorological elements. Therefore, separating the impacts of aerosols on clouds is critical. In addition, although some regional and global numerical models can be used to understand the nature of aerosol-cloud interactions over the TP, the reliability of these simulations is limited by model uncertainties due to the coarse resolution of available data and the parameterization of physical processes.

In the future, more high-quality observations, especially ground-based measurements of aerosol-cloud interactions, are needed. In addition, international cooperation is necessary for studies regarding aerosol-cloud interactions over the TP. Finally, regarding cloud microphysics over the TP, ground-based observations based on national programs could improve our understanding of aerosol-cloud interactions over the TP in the coming decades.

Declaration of Competing Interest

No.

Data availability

Data will be made available on request.

Acknowledgements

This work has been supported by the Second Tibetan Plateau Scientific Expedition and Research Program (STEP) (Grant No. 2019QZKK0602) and jointly supported by the National Natural Science Foundation of China (91937302).

References

Ackerman, A., Toon, O., Stevens, D., Heymsfield, A., Ramanathan, V., Welton, E., 2000. Reduction of tropical cloudiness by soot. Science 288 (5468), 1042–1047.
Adhikari, P., Mejia, J., 2021. Influence of aerosols on clouds, precipitation and freezing level height over the foothills of the Himalayas during the indian summer monsoon. Clim. Dyn. 57, 395–413.
Ban-Weiss, G., Cao, L., Bala, G., Caldeira, K., 2012. Dependence of climate forcing and response on the altitude of black carbon aerosols. Clim. Dyn. 38, 897–911.
Bi, J., Huang, J., Fu, Q., Wang, X., Shi, J., Zhang, W., Huang, Z., Zhang, B., 2011. Toward characterization of the aerosol optical properties over loess plateau of Northwestern China. J. Quant. Spectrosc. Ra. 112, 346–360.
Bian, J., Li, D., Bai, Z., Li, Q., Lv, D., Zhou, X., 2020. Transport of asian surface pollutants to the global stratosphere from the Tibetan Plateau region during the Asian summer monsoon. Natl. Sci. Rev. 7 (3), 516–533.
Boos, W., Kuang, Z., 2010. Dominant control of the South Asian monsoon by orographic insulation versus plateau heating. Nature 436, 218–222.
Bossolasco, A., Jegou, F., Sellitto, P., Berthet, G., Kloss, C., Legras, B., 2021. Global modeling studies of composition and decadal trends of the Asian Tropopause Aerosol Layer. Atmos. Chem. Phys. 21, 2745–2764.
Boucher, O., Randall, D., Artaxo, P., et al., 2013. Clouds and Aerosols. In: [Stocker, T., Qin, D., Plattner, G.-K., et al. (Eds.), Climate Change 2013: The Physical Science Basis. Contribution of Working Group I to the Fifth Assessment Report of the Intergovernmental Panel on Climate Change. Cambridge University Press, Cambridge, United Kingdom and New York, NY, USA, pp. 571–657.
Cai, S., Huang, A., Zhu, K., Yang, B., Yang, X., Wu, Y., Mu, X., 2021. Diurnal cycle of summer precipitation over the Eastern Tibetan Plateau and surrounding regions simulated in a convection-permitting model. Clim. Dyn. 57, 611–632.
Chang, Y., Guo, X., Tang, J., Lu, G., 2019. Aircraft measurement campaign on summer cloud microphysical properties over the Tibetan Plateau. Sci. Rep. 9 (1), 4912.
Charlson, R., Schwartz, S., Hales, J., Cess, R., Coakley, J., Hansen, J., Hofmann, D., 1992. Climate forcing by anthropogenic aerosols. Science 255 (5043), 423–430.
Che, H., Xia, X., Zhao, H., Dubovik, O., Holben, B., Goloub, P., Cuevas-Agulló, E., Estelles, V., Wang, Y., Zhu, J., Qi, B., Gong, W., Yang, H., Zhang, R., Yang, L., Chen, J., Wang, H., Zheng, Y., Gui, K., Zhang, X., Zhang, X., 2019a. Spatial distribution of aerosol microphysical and optical properties and direct radiative effect from the China Aerosol Remote Sensing Network. Atmos. Chem. Phys. 19, 11843–11864.
Che, H., Gui, K., Xia, X., Wang, Y., Holben, B., Goloub, P., Cuevas-Agulló, E., Wang, H., Zheng, Y., Zhao, H., Zhang, X., 2019b. Large contribution of meteorological factors to inter-decadal changes in regional aerosol optical depth. Atmos. Chem. Phys. 19, 10497–10523.
Chen, B., Liu, X., 2005. Seasonal migration of cirrus clouds over the Asian Monsoon regions and the Tibetan Plateau measured from MODIS/Terra. Geophys. Res. Lett. 32, L01804.
Chen, J., Wu, Z., Wu, G., Gong, X., Wang, F., Chen, J., 2021. Ice-nucleating particle concentrations and sources in rainwater over the third pole, Tibetan Plateau. J. Geophys. Res. Atmos. 126 e2020JD033864.
Chen, S., Huang, J., Li, J., Jia, R., Jiang, N., Kang, L., Ma, X., Xie, T., 2017b. Comparison of dust emissions, transport, and deposition between the Taklimakan Desert and Gobi Desert from 2007 to 2011. Sci. China Earth Sci. 60, 1338–1355.
Chen, S., Huang, H., Zhao, C., Qian, Y., Leung, L., Yang, B., 2013. Modeling the transport and radiative forcing of Taklimakan dust over the Tibetan Plateau: a case study in the summer of 2006. J. Geophys. Res. Atmos. 118, 797–812.
Chen, J., Wu, X., Yin, Y., Huang, Q., Xiao, H., 2017a. Characteristics of cloud systems over the Tibetan Plateau and East China during boreal summer. J. Clim. 30 (9), 3117–3137.
Coakley, J., Baldwin, D., 1984. Toward the objective analysis of clouds from satellite imagery data. J. Clim. Appl. Meteorol. 23, 1065–1099.
Cong, Z., Kang, S., Smirnov, A., Holben, B., 2009. Aerosol optical properties at nam co, a remote site in central Tibetan Plateau. Atmos. Res. 92 (1), 42–48.
Cong, Z., Kang, S., Gao, S., Zhang, Y., Li, Q., Kawarmura, K., 2013. Historical trends of atmospheric black carbon on Tibetan Plateau as reconstructed from a 150-year lake sediment record. Environ. Sci. Technol. 47 (6), 2579–2586.
Cong, Z., Kang, S., Liu, X., Wang, G., 2007. Elemental composition of aerosol in the Nam co region, Tibetan Plateau, during summer monsoon season. Atmos. Environ. 41 (6), 1180–1187.
Cotton, W., Yuter, S., 2009. Principles of Cloud and Precipitation Formation. Springer, Netherlands.
Duan, A., Liu, S., Zhao, Y., Gao, K., Hu, W., 2018. Atmospheric heat source/sink dataset over the Tibetan Plateau based on satellite and routine meteorological observations. Big Earth Data 2, 179–189.
Duan, A., Xiao, Z., 2015. Does the climate warming hiatus exist over the Tibetan Plateau. Sci. Rep. 5, 13711.
Duan, A., Li, F., Wang, M., Wu, G., 2011. Persistent weakening trend in the spring sensible heat source over the Tibetan Plateau and its impact on the Asian summer monsoon. J. Clim. 24, 5671–5682.
Duan, A., Wu, G., 2006. Change of cloud amount and the climate warming on the Tibetan Plateau. Geophys. Res. Lett. 33, L22704.
Duo, B., Zhang, Y., Kong, L., Fu, H., Hu, Y., Chen, J., Li, L., Qiong, A., 2015. Individual particle analysis of aerosols collected at Lhasa city in the Tibetan Plateau. J. Environ. Sci. 29, 165–177.
Fadnavis, S., Roy, C., Sabin, T., Ayantika, D., Ashok, K., 2017. Potential modulations of pre-monsoon aerosols during Elnino: impact on Indian summer monsoon. Clim. Dyn. 49, 2279–2290.
Fadnavis, S., Semeniuk, K., Pozzoli, L., Schultz, M.G., Ghude, S.D., Das, S., Kakatkar, R., 2013. Transport of aerosols into the UTLS and their impact on the Asian monsoon region as seen in a global model simulation. Atmos. Chem. Phys. 13, 8771–8786.
Fang, K., Makkonen, R., Guo, Z., Zhao, Y., Seppa, H., 2015. An increase in the biogenic aerosol concentration as a contributing factor to the recent wetting trend in Tibetan Plateau. Sci. Rep. 5, 14628.
Feng, L., Zhou, T., 2012. Water vapor transport for summer precipitation over the Tibetan Plateau: multi-dataset analysis. J. Geophys. Res. Atmos. 117, D20114.
Feng, X., Mao, R., Gong, D., Zhao, C., Wu, C., Zhao, C., Wu, G., Lin, Z., Liu, X., Wang, K., Sun, Y., 2020. Increased dust aerosols in the high troposphere over the Tibetan Plateau from 1990s to 2000s. J. Geophys. Res. Atmos. 125 (13).
Forster, P., Storelvmo, T., Armour, K., et al., 2021. The Earth's Energy Budget, Climate Feedbacks, and Climate Sensitivity. In *Climate Change 2021: The Physical Science Basis. Contribution of Working Group I to the Sixth Assessment Report of the Intergovernmental Panel on Climate Change* [Masson-Delmotte. Cambridge University Press, Cambridge, United Kingdom and New York, NY, USA, pp. 923–1054.
Fu, R., Hu, Y., Wright, J.S., Jiang, J.H., Dickinson, R.E., Chen, M., Filipiak, M., Read, W. G., Waters, J.W., Wu, D.L., 2006. Short circuit of water vapor and polluted air to the global stratosphere by convective transport over the Tibetan Plateau. Proc. Natl. Acad. Sci. U. S. A. 103 (15), 5664–5669.
Fujinami, H., Yasunari, T., 2001. The seasonal and intraseasonal variability of diurnal cloud activity over the Tibetan Plateau. J. Meteor. Soc. Japan 79 (6), 1207–1227.
Gao, B.C., Yang, P., Guo, G., Park, S.K., Wiscombe, W.J., Chen, B., 2003. Measurements of water vapor and high clouds over the Tibetan Plateau with the Terra MODIS instrument. IEEE Trans. Geosci. Remote Sens. 41 (4), 895–900.
Garrett, T., Zhao, C., 2006. Increased Arctic cloud longwave emissivity associated with pollution from mid-latitudes. Nature 440, 787–789.
Ge, J., Wang, Z., Liu, Y., Su, J., Dong, Z., 2019. Linkages between mid-latitude cirrus cloud properties and large-scale meteorology at the SACOL site. Clim. Dyn. 53, 5035–5046.
Ge, J., Zheng, C., Xie, H., Xin, Y., Huang, J., Fu, Q., 2018. Midlatitude cirrus clouds at the SACOL Site: macrophysical properties and large-scale atmospheric states. J. Geophys. Res. Atmos. 123 (4), 2256–2271.
Ge, J., Zhu, Z., Zheng, C., Xie, H., Zhou, T., Huang, J., Fu, Q., 2017. An improved hydrometeor detection method formillimeter-wavelength cloud radar. Atmos. Chem. Phys. 17 (14), 9035–9047.
Ge, J., Huang, J., Xu, C., Qi, Y., Liu, H., 2014. Characteristics of Taklimakan dust emission and distribution: a satellite and reanalysis field perspective. J. Geophys. Res. Atmos. 119, 11772–11783.
Han, Y., Fang, X., Zhao, T., et al., 2009. Suppression of precipitation by dust particles originated in the Tibetan Plateau. Atmos. Environ. 43 (3), 569–574.
Hartmann, D., Ockert-Bell, M., Michelson, M., 1992. The effect of cloud type on earth's energy balance: Global analysis. J. Clim. 5 (10), 1157–1171.
He, Q., Li, C., Ma, J., Wang, H., Shi, G., Liang, Z., Luan, Q., Geng, F., Zhou, X., 2013. The properties and formation of cirrus clouds over the Tibetan plateau based on summertime Lidar measurements. J. Atmos. Sci. 70 (3), 901–915.
He, Y., Tian, W., Huang, J., Wang, G., Ren, Y., Yan, H., Yu, H., Guan, X., Hu, H., 2021. The mechanism of increasing summer water vapor over the Tibetan Plateau. J. Geophys. Res. Atmos. 126 e2020JD034166.

Hu, L., Yang, S., Li, Y., Gao, S., 2010. Diurnal variability of precipitation depth over the Tibetan Plateau and its surrounding regions. Adv. Atmos. Sci. 27 (1), 115–122.
Hu, Z., Huang, J., Zhao, C., Jin, Q., Ma, Y., Yang, B., 2020. Modeling dust sources, transport, and radiative effects at different altitudes over the Tibetan Plateau. Atmos. Chem. Phys. 20, 1507–1529.
Hua, S., Liu, Y., Luo, R., Shao, T., Zhu, Q., 2020. Inconsistent aerosol indirect effects on water clouds and ice clouds over the Tibetan Plateau. Int. J. Climatol. 40 (8), 3832–3848.
Hua, S., Liu, Y., Jia, R., Chang, S., Wu, C., Zhu, Q., Shao, T., Wang, B., 2018. Role of clouds in accelerating cold-season warming during 2000–2015 over the Tibetan Plateau. Int. J. Climatol. 38 (13), 4950–4966.
Huang, J., Minnis, P., Yan, H., Yi, Y., Chen, B., Zhang, L., Ayers, J.K., 2010. Dust aerosol effect on semi-arid climate over Northwest China detected from A-Train satellite measurements. Atmos. Chem. Phys. 10, 6863–6872.
Huang, J., Minnis, P., Yi, Y., Tang, Q., Wang, X., Hu, Y., Liu, Z., Ayers, K., Trepte, C., Winker, D., 2007. Summer dust aerosols detected from CALIPSO over the Tibetan Plateau. Geophys. Res. Lett. 34 (18).
Huang, J., Wang, Y., Wang, T., Yi, Y., 2006. Dusty cloud radiative forcing derived from satellite data for middle latitude regions of East Asia. Prog. Nat. Sci. 16 (10), 1084–1089.
Huang, J., Minnis, P., Lin, B., Wang, T., Yi, Y., Hu, Y., Sun-Mack, S., Ayers, K., 2006b. Possible influences of asian dust aerosols on cloud properties and radiative forcing observed from MODIS and CERES. Geophys. Res. Lett. 33 (6).
Immerzeel, W., Van Beek, L., Bierkens, M., 2010. Climate change will affect the Asian water towers. Science 328 (5984), 1382–1385.
Jacobson, M.Z., 2002. Analysis of aerosol interactions with numerical techniques for solving coagulation, nucleation, condensation, dissolution, and reversible chemistry among multiple size distributions. J. Geophys. Res. 107 (D19), 4366.
Ji, Z., Kang, S., Cong, Z., Zhang, Q., Yao, T., 2015. Simulation of carbonaceous aerosols over the Third Pole and adjacent regions: distribution, transportation, deposition, and climatic effects. Clim. Dyn. 45, 2831–2846.
Jia, R., Luo, M., Liu, Y., Zhu, Q., Hua, S., Wu, C., Shao, T., 2019. Anthropogenic aerosol pollution over the eastern slope of the Tibetan Plateau. Adv. Atmos. Sci. 36, 847–862.
Jia, R., Liu, Y., Hua, S., Zhu, Q., Shao, T., 2018. Estimation of the aerosol radiative effect over the Tibetan Plateau based on the latest CALIPSO product. J. Meteor. Res. 32 (5), 707–722.
Jia, R., Liu, Y., Chen, B., Zhang, Z., Huang, J., 2015. Source and transportation of summer dust over the Tibetan Plateau. Atmos. Environ. 123, 210–219.
Jiang, Y., Yang, X.-Q., Liu, X., Yang, D., Sun, X., Wang, M., Ding, A., Wang, T., Fu, C., 2017. Anthropogenic aerosol effects on East Asian winter monsoon: the role of black carbon-induced Tibetan Plateau warming. J. Geophys. Res. Atmos. 122, 5883–5902.
Kang, L., Huang, J., Chen, S., Wang, X., 2016. Long-term trends of dust events over Tibetan Plateau during 1961–2010. Atmos. Environ. 125, 188–198.
Kang, S., Wake, C., Dahe, Q., Mayewski, A., Tandong, Y., 2000. Monsoon and dust signals recorded in Dasuopu glacier, Tibetan Plateau. J. Glaciol. 46, 222–226.
Lau, K.-M., Yuan, C., Li, Z., 2018. Origin, maintenance and variability of the Asian Tropopause Aerosol Layer (ATAL): the roles of monsoon dynamics. Sci. Rep. 8 (1), 3960.
Lau, K.-M., Kim, K., 2010. Fingerprinting the impacts of aerosols on long-term trends of the Indian summer monsoon regional rainfall. Geophys. Res. Lett. 37, 127–137.
Lau, K.-M., Ramanathan, V., Wu, G.-X., Li, Z., Tsay, S.C., Hsu, C., Sikka, R., Holben, B., Lu, D., Tartari, G., Chin, M., Koudelova, P., Chen, H., Ma, Y., Huang, J., Taniguchi, K., Zhang, R., 2008. The joint aerosol-monsoon experiment: a new challenge for monsoon climate research. Bull. Amer. Meteor. Soc. 89 (3), 369–383.
Lau, K.-M., Kim, K.M., 2006. Asian summer monsoon anomalies induced by aerosol direct forcing: the role of the Tibetan Plateau. Clim. Dyn. 26, 855–864.
Lei, Y., Letu, H., Shang, H., Shi, J., 2020. Cloud cover over the Tibetan Plateau and eastern China: a comparison of ERA5 and ERA-interim with satellite observations. Clim. Dyn. 54, 2941–2957.
Levin, Z., Cotton, W.R., 2007. Aerosol Pollution Impact on Precipitation: A Scientific Review. World Meteorological Organization, Geneva, Switzerland.
Li, F., Wan, X., Wang, H., Orsolini, Y.J., Cong, Z., Gao, Y., Kong, S., 2020. Arctic Sea-ice loss intensifies aerosol transport to the Tibetan Plateau. Nat. Clim. Chang. 10, 1037–1044.
Li, Q., Jiang, J.H., Wu, D.L., Read, W.G., Livesey, N.J., Jacob, D.J., 2005. Convective outflow of South Asian pollution: a global CTM simulation compared with EOS MLS observations. Geophys. ResLett 32.
Li, X., Kang, S., He, X., Qu, B., Tripathee, L., Jing, Z., Paudyal, R., Li, Y., Zhang, Y., Yan, F., Li, G., Li, C., 2017. Light-absorbing impurities accelerate glacier melt in the central Tibetan Plateau. Sci. Total Environ. 587, 482–490.
Li, Y., Liu, X., Chen, B., 2006. Cloud type climatology over the Tibetan Plateau: a comparison of ISCCP and MODIS/TERRA measurements with surface observations. Geophys. Res. Lett. 33, L17716.
Li, Y., Zhang, M., 2016. Cumulus over the Tibetan Plateau in the Summer based on CloudSat–CALIPSO Data. J. Clim. 29 (3), 1219–1230.
Li, Y., Wang, Y., Song, Y., Hu, L., Gao, S., Rong, F., 2008. Characteristics of summer convective systems initiated over the Tibetan Plateau. Part I: Origin, track, development, and precipitation. J. Appl. Meteorol. Climatol. 47, 2679–2695.
Liou, K., 1986. Influence of cirrus clouds on weather and climate processes: a global perspective. Mon. Weather Rev. 114, 1167–1199.
Liu, D., Wang, Z., Liu, Z., Winker, D., Trepte, C., 2008. A height resolved global view of dust aerosols from the first year CALIPSO lidar measurements. J. Geophys. Res. Atmos. 113 (D16), D16214.
Liu, L., Feng, J., Chu, R., Zhou, Y., Ueno, K., 2002. The diurnal variation of precipitation in monsoon season in the Tibetan Plateau. Adv. Atmos. Sci. 19, 365–378.
Liu, Y., Zhu, Q., Hua, S., Alam, K., Dai, T., Cheng, Y., 2020. Tibetan Plateau driven impact of Taklimakan dust on northern rainfall. Atmos. Environ. 234, 117583.
Liu, Y., Hua, S., Jia, R., Huang, J., 2019a. Effect of aerosols on the ice cloud properties over the Tibetan Plateau. J. Geophys. Res. Atmos. 124, 9594–9608.
Liu, Y., Zhu, Q., Wang, R., Xiao, K., Cha, P., 2019b. Distribution source and transport of the aerosols over Central Asia. Atmos. Environ. 210, 120–131.
Liu, Y., Sato, Y., Jia, R., Xie, Y., Huang, J., Nakajima, T., 2015. Modeling study on the transport of summer dust and anthropogenic aerosols over the Tibetan Plateau. Atmos. Chem. Phys. 15, 12581–12594.
Liu, Y., Huang, J., Shi, G., Takamura, T., Khatri, P., Bi, J., Shi, J., Wang, T., Wang, X., Zhang, B., 2011. Aerosol optical properties and radiative effect determined from sky-radiometer over Loess Plateau of Northwest China. Atmos. Chem. Phys. 11, 11455–11463.
Luo, H., Yanai, M., 1984. The large-scale circulation and heat sources over the Tibetan Plateau and surrounding areas during the early summer of 1979. Part II: Heat and moisture budgets. Mon. Wea. Rev. 112, 966–989.
Luo, M., Liu, Y., Zhu, Q., Tang, Y., Alam, K., 2020. Role and mechanisms of black carbon affecting water vapor transport to Tibet. Remote Sens. 12 (2), 231.
Luo, Y., Zhang, R., Qian, W., Luo, Z., Hu, X., 2011. Intercomparison of deep convection over the Tibetan Plateau-Asian monsoon region and subtropical North America in boreal summer using CloudSat/CALIPSO data. J. Clim. 24, 2164–2177.
Ma, J., Brühl, C., He, Q., Steil, B., Karydis, V.A., Klingmülle, K., Tost, H., Chen, B., Jin, Y., Liu, N., Xu, X., Yan, P., Zhou, X., Abdelrahman, K., Pozzer, A., Lelieveld, J., 2019. Modeling the aerosol chemical composition of the tropopause over the Tibetan Plateau during the Asian summer monsoon. Atmos. Chem. Phys. 19 (17), 11587–11612.
Ma, Y., Ma, W., Zhong, L., Hu, Z., Li, M., Zhu, Z., Han, C., Wang, B., Liu, X., 2017. Monitoring and modeling the Tibetan Plateau's climate system and its impact on East Asia. Sci. Rep. 7, 44574.
Ma, Y., Lu, M., Chen, H., Pan, M., Hong, Y., 2018. Atmospheric moisture transport versus precipitation across the Tibetan Plateau: a mini-review and current challenges. Atmos. Res. 209, 50–58.
Mehta, M., Khushboo, R., Raj, R., Singh, N., 2021. Spaceborne observations of aerosol vertical distribution over Indian mainland (2009–2018). Atmos. Environ. 244, 117902.
Miller, R.L., Tegen, I., 1998. Climate response to soil dust aerosols. J. Clim. 11, 3247–3267.
Mills, M., Toon, O., Lee-Taylor, J., Robock, A., 2014. Multidecadal global cooling and unprecedented ozone loss following a regional nuclear conflict. Earths Future 2 (4), 161–176.
Molnar, P., Boos, W., Battisti, D., 2010. Orographic controls on climate and paleoclimate of Asia: thermal and mechanical rolesfor the Tibetan Plateau. Annu. Rev. Earth Pl. Sc. 38 (1), 77–102.
Naud, C., Chen, Y., 2010. Assessment of ISCCP cloudiness over the Tibetan Plateau using CloudSat-CALIPSO. In: J. Geophys. Res, Atmos, p. 115.
Niu, H., Kang, S., Gao, W., Wang, Y., Paudyal, R., 2019. Vertical distribution of the Asian tropopause aerosols detected by CALIPSO. Environ. Pollut. 253, 207–220.
Pan, B., Yao, Z., Wang, M., Pan, H., Bu, L., Kumar, K., Gao, H., Huang, X., 2018. Evaluation and utilization of CloudSat and CALIPSO data to analyze the impact of dust aerosol on the microphysical properties of cirrus over the Tibetan Plateau. Adv. Space Res. 63 (1), 2–15.
Pan, L., Honomichl, S., Kinnison, D., Abalos, M., Randel, W., Bergman, J., Bian, J., 2016. Transport of chemical tracers from the boundary layer to stratosphere associated with the dynamics of the Asian summer monsoon. J. Geophys. Res. Atmos. 121, 14159–14174.
Penner, J.E., Hegg, D., Leaitch, R., 2001. Unraveling the role of aerosols in climate change. Environ. Sci. Technol. 35, 332–340.
Qian, Y., Flanner, M., Leung, L., Wang, W., 2011. Sensitivity studies on the impacts of Tibetan Plateau snowpack pollution on the Asian hydro- logical cycle and monsoon climate. Atmos. Chem. Phys. 11, 1929–1948.
Qie, X., Wu, X., Yuan, T., Bian, J., Lu, D., 2014. Comprehensive pattern of deep convective systems over the Tibetan Plateau-South Asian monsoon region based on TRMM data. J. Clim. 27 (17), 6612–6626.
Qin, D., Mayewski, P., Wake, C., Kang, S., Ren, J., 2000. Evidence for recent climate change from ice cores in the Central Himalayas. Ann. Glaciol. 31, 153–158.
Ramanathan, V., Crutzen, P.J., Kiehl, J.T., Rosenfeld, D., 2001. Aerosols, climate, and the hydrological cycle. Science 294 (5549), 2119–2124.
Ramanathan, V., Cess, R.D., Harrison, E.F., Minnis, P., Barkstrom, B.R., Ahmad, E., Hartmann, D., 1989. Cloud radiative forcing and climate: results from the Earth Radiation Budget Experiment. Science 243 (4887), 57–63.
Rosenfeld, D., Sherwood, S., Wood, R., Leo, D., 2014. Climate effects of aerosol-cloud interactions. Science 343, 379–380.
Rossow, W., Schiffer, R., 1999. Advances in understanding clouds from ISCCP. Bull. Am. Meteorol. Soc. 80, 2261–2287.
Rüthrich, F., Thies, B., Reudenbach, C., Bendix, J., 2013. Cloud detection and analysis on the Tibetan Plateau using Meteosat and CloudSat. J. Geophys. Res. Atmos. 118, 10082–10099.
Samset, B.H., Myhre, G., 2015. Climate response to externally mixed black carbon as a function of altitude. J. Geophys. Res. Atmos. 120 (7), 2913–2927.
Sato, T., Yoshikane, T., Satoh, M., Miltra, H., Fujinami, H., 2008. Resolution dependency of the diurnal cycle of convective clouds over the Tibetan Plateau in a mesoscale model. J. Meteor. Soc. Japan 86A, 17–31.
Sato, T., Miura, H., Satoh, M., 2007. Spring diurnal cycle of clouds over Tibetan Plateau: global cloud-resolving simulations and satellite observations. Geophys. Res. Lett. 34 (18).

Shang, H., Letu, H., Nakajima, T.Y., Wang, Z., Ma, R., Wang, T., Lei, Y., Ji, D., Li, S., Shi, J., 2018. Diurnal cycle and seasonal variation of cloud cover over the Tibetan Plateau as determined from Himawari-8 new-generation geostationary satellite data. Sci. Rep. 8, 1105.

Slingo, A., 1989. A GCM parameterization for the shortwave radiative properties of water clouds. J. Atmos. Sci. 46 (10), 1419–1427.

Solomon, S., Daniel, J.S., Neely, R.R., Vernier, J.-P., Dutton, E.G., Thomason, L.W., 2011. The persistently variable "background" stratospheric aerosol layer and global climate change. Science 333 (6044), 866–870.

Sohn, B., Nakajima, T., Satoh, M., Jang, H., 2010. Impact of different definitions of clear-sky flux on the determination of longwave cloud radiative forcing: NICAM simulation results. Atmos. Chem. Phys. 10, 11641.

Su, W., Mao, J., Ji, F., Qin, Y., 2000. Outgoing longwave radiation and cloud radiative forcing of the Tibetan Plateau. J. Geophys. Res. 105 (D11), 14863.

Sun, Z., 1995. Comparison of observed and modelled radiation budget over the Tibetan Plateau using satellite data. Int. J. Climatol. 15 (4), 423–445.

Tan, Z., Liu, Y., Zhu, Q., Shao, T., 2021. Impact of massive topography on the dust cycle surrounding the Tibetan Plateau. Atmos. Environ. 264, 118703.

Thulasiraman, S., O'Neill, N.T., Royer, A., Holben, B.N., Westphal, D.L., McArthur, L.J. B., 2002. Sunphotometric observations of the 2001 Asian dust storm over Canada and the U.S. Geophys. Res. Lett. 29 (8), 96-1-96-4.

Tobo, Y., Iwasaka, Y., Shi, G.Y., Kim, Y.S., Ohashi, T., Tamura, K., Zhang, D., 2007. Balloon-borne observations of high aerosol concentrations near the summertime tropopause over the Tibetan Plateau. Atmos. Res. 84 (3), 233–241.

Twomey, S.A., Piepgrass, M., Wolfe, T.L., 1984. An assessment of the impact of pollution on global cloud albedo. Tellus B 36 (5), 356–366.

Twomey, S.A., 1977. The influence of pollution on the shortwave albedo of clouds. J. Atmos. Sci. 34 (7), 1149–1154.

Twomey, S., 1974. Pollution and the planetary albedo. Atmos. Environ. 8 (12), 1251–1256.

Ueno, K., Fujii, H., Yamada, H., Liu, L., 2001. Weak and frequent monsoon precipitation over the Tibetan Plateau. J. Meteor. Soc. Japan 79 (1B), 419–434.

Ueno, K., 1998. Characteristics of plateau-scale precipitation in Tibet estimated by satellite data during 1993 monsoon season. J. Meteor. Soc. Japan 76, 533–548.

Uno, I., Amano, H., Emori, S., Kinoshita, K., Matsui, I., Sugimoto, N., 2001. Trans-Pacific yellow sand transport observed in April 1998: a numerical simulation. J. Geophys. Res. 106 (D16), 18331–18344.

Uyeda, H., Yamada, H., Horikomi, J., Shirooka, R., Shimizu, S., Liu, L., Ueno, K., Fujii, H., Koike, T., 2001. Characteristics of convective clouds observed by a Doppler Radar at Naqu on Tibetan Plateau during the GAME-Tibet IOP. J. Meteor. Soc. Japan 79 (1B), 463–474.

Vernier, J.-P., Fairlie, T.D., Natarajan, M., Wienhold, F.G., Bian, J., Martinsson, B.G., Crumeyrolle, S., Thomason, L.W., Bedka, K.M., 2015. Increase in upper tropospheric and lower stratospheric aerosol levels and its potential connection with asian pollution. J. Geophys. Res. Atmos. 120 (4), 1608–1619.

Wan, B., Gao, Z., Chen, F., Lu, C., 2017. Impact of Tibetan Plateau surface heating on persistent extreme precipitation events in Southeastern China. Mon. Weather Rev. 145 (9), 3485–3505.

Wang, B., Bao, Q., Hoskins, B., Wu, G., Liu, Y., 2008. Tibetan Plateau warming and precipitation changes in East Asia. Geophys. Res. Lett. 35 (14).

Wang, J., Jian, B., Wang, G., Zhao, Y., Li, Y., Letu, H., Zhang, M, Li, J., 2021a. Climatology of Cloud Phase, Cloud Radiative Effects and Precipitation Properties over the Tibetan Plateau. Remote Sens. 13, 363.

Wang, T., Han, Y., Hua, W., Tang, J., Huang, J., Zhou, T., Huang, Z., Bi, J., Xie, H., 2021b. Profiling dust mass concentration in Northwest China using a joint lidar and sun-photometer setting. Remote Sens. 13 (6), 1099.

Wang, N., Yao, T., Thompson, L., Davis, M., 2006. Strong negative correlation between dust event frequency and air temperature over the northern Tibetan Plateau reflected by the Malan ice-core record. Ann. Glaciol. 43, 29–33.

Wang, T., Chen, Y., Gan, Z., Han, Y., Li, J., Huang, J., 2020. Assessment of dominating aerosol properties and their long-term trend in the Pan-Third Pole region: a study with 10-year multi-sensor measurements. Atmos. Environ. 239, 117738.

Wang, X., Huang, J., Zhang, R., Chen, B., Bi, J., 2010. Surface measurements of aerosol properties over Northwest China during ARM China 2008 deployment. J. Geophys. Res. Atmos. 115, D00K27.

Wang, Y., Khalizov, A., Levy, M., Zhang, R., 2013. New Directions: Light absorbing aerosols and their atmospheric impacts. Atmos. Environ. 81, 713–715.

Wu, G., Duan, A., Liu, Y., Mao, J., Ren, R., Bao, Q., He, B., Liu, B., Hu, W., 2015. Tibetan Plateau climate dynamics: recent research progress and outlook. Natl. Sci. Rev. 2 (1), 100–116.

Wu, G., Liu, Y., Dong, B., Liang, X., Duan, A., Bao, Q., Yu, J., 2012. Revisiting Asian monsoon formation and change associated with Tibetan plateau forcing: Iformation. Clim. Dyn. 39 (5), 1169–1181.

Wu, G., Liu, Y., Zhang, Q., Duan, A., Wang, T., Wan, R., Liu, X., Li, W., Wang, Z., Liang, X., 2007. The influence of mechanical and thermal forcing by the Tibetan Plateau on Asian climate. J. Hydro. Meteor. Spec. Sect. 8 (4), 770–789.

Wu, G., Zhang, Y., 1998. Tibetan Plateau forcing and the timing of the monsoon onset over South Asia and the South China Sea. Mon. Wea. Rev. 126, 913–927.

Xia, X., Wang, P., Wang, Y., Li, Z., Xin, J., Liu, J., et al., 2008. Aerosol optical depth over the Tibetan Plateau and its relation to aerosols over the Taklimakan Desert. Geophys. Res. Lett. 35, L16804.

Xu, C., Ma, Y., You, C., Zhu, Z., 2015. The regional distribution characteristics of aerosol optical depth over the Tibetan Plateau. Atmos. Chem. Phys. 15 (20), 12065–12078.

Xu, C., Ma, Y., Yang, K., You, C., 2018. Tibetan Plateau impacts on global dust transport in the upper troposphere. J. Clim. 31 (12), 4745–4756.

Xu, J., Hou, S., Qin, D., Kang, S., Ren, J., Ming, J., 2007. Dust storm activity over the Tibetan Plateau recorded by a shallow ice core from the north slope of Mt. Qomolangma (Everest), Tibet-Himal region. Geophys. Res. Lett. 34, L17504.

Xu, X., Lu, C., Ding, Y., Shi, X., Guo, Y., Zhu, W., 2013. What is the relationship between China summer precipitation and the change of apparent heat source over the Tibetan Plateau? Atmos. Sci. Lett. 14, 227–234.

Xu, X., Lu, C., Shi, X., Gao, S., 2008. World water tower: an atmospheric perspective. Geophys. Res. Lett. 35 (20).

Xu, X., Xie, L., Yang, X., et al., 2020. Aerosol optical properties at seven AERONET sites over Middle East and Eastern Mediterranean Sea. Atmos. Environ. 243, 117884.

Xu, X., Zhou, M., Chen, J., Bian, L., Zhang, G., Liu, H., Li, S., Zhang, H., Zhao, Y., Suolongduoji, Wang, J., 2002. A comprehensive physical pattern of land-air dynamic and thermal structure on the Qinghai-Xizang Plateau. Sci. China Ser. D-Earth Sci. 45 (7), 577–594.

Xu, Y., Gao, Y., 2019. Quantification of evaporative sources of precipitation and its changes in the Southeastern Tibetan Plateau and Middle Yangtze River Basin. Atmos. 10 (8).

Yan, H., Huang, J., He, Y., Liu, Y., Wang, T., Li, J., 2020. Atmospheric water vapor budget and its long-term trend over the Tibetan Plateau. J. Geophys. Res. Atmos. 125 e2020JD033297.

Yan, Y., Liu, Y., Lu, J., 2016. Cloud vertical structure, precipitation, and cloud radiative effects over Tibetan Plateau and its neighboring regions. J. Geophys. Res. Atmos. 121, 5864–5877.

Yanai, M., Li, C., Song, Z., 1992. Seasonal heating of the Tibetan Plateau and its effects on the evolution of the Asian summer monsoon. J. Meteor. Soc. Japan 70, 319–351.

Yang, F., He, Q., Huang, J., Mamtimin, A., Yang, X., Huo, W., Zhou, C., Liu, X., Wei, W., Cui, C., Wang, M., Li, H., Yang, L., Zhang, H., Liu, Y., Zheng, Xin, Pan, H., Jin, Li, Zou, H., Zhou, L., Liu, Y., Zhang, J., Meng, L., Wang, Y., Qin, X., Yao, Y., Liu, H., Xue, F., Zheng, W., 2021. Desert environment and climate observation network over the Taklimakan Desert. B. Am. Mete. Orol, Soc. 102 (6). E1172–E1191.

Yang, J., Wang, W.-C., Chen, G., Bao, Q., Qi, X., Zhou, S., 2018. Intraseasonal variation of the black carbon aerosol concentration and its impact on atmospheric circulation over the southeastern Tibetan Plateau. J. Geophys. Res. Atmos. 123 (19), 10881–10894.

Yang, K., Wu, H., Qin, J., Lin, C., Tang, W., Chen, Y., 2014. Recent climate changes over the Tibetan Plateau and their impacts on energy and water cycle: a review. Glob. Planet. Change 112, 79–91.

Yang, K., Ding, B., Qin, J., Tang, W., Lu, N., Lin, C., 2012. Can aerosol loading explain the solar dimming over the Tibetan Plateau? Geophys. Res. Lett. 39, L20710.

Yao, T., Thompson, L., Yang, W., Yu, W., Gao, Y., Guo, X., Yang, X., Duan, K., Zhao, H., Xu, B., Pu, J., Lu, A., Yang, X., Kattel, D., Joswiak, D., 2012. Different glacier status with atmospheric circulations in Tibetan Plateau and surroundings. Nat. Clim. Chang. 2, 663–667.

Yasunori, K., Fujio, K., 2002. Relationship between topography and daytime cloud activity around Tibetan Plateau. J. Meteor. Soc. Japan 80 (6), 1339–1355.

You, Q., Jiao, Y., Lin, H., Min, J., Kang, S., Ren, G., Meang, X., 2014. Comparison of NCEP/NCAR and ERA-40 total cloud cover with surface observations over the Tibetan Plateau. Int. J. Climatol. 34, 2529–2537.

Yu, P., Rosenlof, K., Shang, L., Telg, H., Gao, R., 2017. Efficient transport of tropospheric aerosol into the stratosphere via the Asian summer monsoon anticyclone. Proc. Natl. Acad. Sci. U. S. A. 114 (27), 6972–6977.

Yu, P., Murphy, D., Portmann, R., Toon, O., Froyd, K., Rollins, A., Gao, R., Rosenlof, K., 2016. Radiative forcing from anthropogenic sulfur and organic emissions reaching the stratosphere. Geophys. Res. Lett. 43, 9361–9367.

Yu, R., Wang, B., Zhou, T., 2004. Climate effects of the deep continental stratus clouds generated by the Tibetan Plateau. J. Clim. 17 (13), 2702–2713.

Yuan, C., Lau, K.-M., Li, Z., Cribb, M., Wang, T., et al., 2019. Relationship between Asian monsoon strength and transport of surface aerosols to the Asian Tropopause Aerosol Layer (ATAL): Interannual variability and decadal changes. Atmos. Chem. Phys. 19 (3), 1901–1913.

Yuan, T., Chen, S., Wang, L., Yang, Y., Bi, H., Zhang, X., Zhang, Y., 2020. Impacts of two East asian atmospheric circulation modes on black carbon aerosol over the Tibetan Plateau in winter. J. Geophys. Res. Atmos. 125 e2020JD032458.

Yumimoto, K., Eguchi, K., Uno, I., Takemura, T., Liu, Z., Shimizu, A., 2009. An elevated large-scale dust veil from the Taklimakan desert: intercontinental transport and three-dimensional structure as captured by CALIPSO and regional and global models. Atmos. Chem. Phys. 9, 8545–8558.

Zelinka, M., Klein, S., Taylor, K., Andrews, T., Webb, M., Gregory, J., Forster, P., 2013. Contributions of different cloud types to feedbacks and rapid adjustments in CMIP5. J. Clim. 26, 5007–5027.

Zhang, C., Tang, Q., Chen, D., 2017. Recent changes in the moisture source of precipitation over the Tibetan Plateau. J. Clim. 30 (5), 1807–1819.

Zhang, J., Xia, X., Shi, H., Zong, X., Li, J., 2020. Radiation and aerosol measurements over the Tibetan Plateau during the asian summer monsoon period. Atmos. Pollut. Res. 11, 1543–1551.

Zhang, L., Tang, C., Huang, J., Du, T., Guang, X., Tian, P., Shi, J., Cao, X., Huang, Z., Guo, Q., Zhang, H., Wang, M., Zeng, H., Wang, F., Dolkar, P., 2021. Unexpected high absorption of atmospheric aerosols over a western Tibetan Plateau site in summer. J. Geophys. Res. Atmos. 126 (7).

Zhang, R., Wang, H., Qian, Y., Rasch, P., Easter, R., Ma, P., Singh, B., Huang, J., Fu, Q., 2015. Quantifying sources, transport, deposition, and radiative forcing of black carbon over the Himalayas and Tibetan Plateau. Atmos. Chem. Phys. 15, 6205–6223.

Zhang, X., Peng, L., Zheng, D., Tao, J., 2008. Cloudiness variations over the Qinghai-Xizang (Tibetan) Plateau during 1971–2004. J. Geogr. Sci. 18, 142–154.

Zhang, X., Arimoto, R., Cao, J., An, Z., Wang, D., 2001. Atmospheric dust aerosol over the Tibetan Plateau: quantifying the radiative impacts of mineral dust (dust). J. Geophys. Res. Atmos. 106, 18471–18476.

Zhao, C., Yang, Y., Fan, H., Huang, J., Fu, Y., Zhang, X., Kang, S., Cong, Z., Husi, L., Massimo, M., 2020. Aerosol characteristics and impacts on weather and climate over the Tibetan Plateau. Natl. Sci. Rev. 7 (3), 492–495.

Zhao, Z., Wang, Q., Xu, B., Shen, Z., Zhuang, R., Zhu, C., Su, X., Zhao, S., Long, X., Liu, S., 2017. Black carbon aerosol and its radiative impact at a high-altitude remote site on the south- eastern Tibet Plateau. J. Geophys. Res. Atmos. 122, 5515–5530.

Zhou, C., Zhao, P., Chen, J., 2019. The interdecadal change of summer water vapor over the Tibetan Plateau and associated mechanisms. J. Clim. 32, 4103–4119.

Zhou, R., Wang, G., Zhaxi, S., 2021. Cloud vertical structure measurements from a ground-based cloud radar over the southeastern Tibetan Plateau. Atmos. Res. 258 (2021), 105629.

Zhou, X., Zhao, P., Chen, J., Chen, L., Li, W., 2009. Impacts of thermodynamic processes over the Tibetan Plateau on the Northern Hemispheric climate. Sci. China Earth Sci. 52, 1679–1693.

Zhou, X., Bei, N., Liu, H., Cao, J., Xing, L., Lei, W., Molina, L., Li, G., 2017. Aerosol effects on the development of cumulus clouds over the tibetan plateau. Atmos. Chem. Phys. 17 (12), 1–31.

Zhu, Q., Liu, Y., Shao, T., Luo, R., Tan, Z., 2021. A simulation study on the new transport pathways of global tropopause dust layer. Geophys. Res. Lett. 48 e2021GL096063.